國立交通大學

物理研究所

碩士論文

太陽微中子之謎

Solar Neutrino Puzzle

研 究 生：蔡岳霖

指導教授：Athar Husain 教授

林貴林 教授

中華民國 93 年七月

Solar Neutrino Puzzle

研 究 生：蔡岳霖　　Student：Yue-Lin Tasi

指導教授：Athar Husain　　Advisor：Athar Husain

林貴林　　Guey-Lin Lin

國立交通大學

物理研究所

碩 士 論 文

A Thesis

Submitted to Institute of Physics

College of Science

National Chiao Tung University

in partial Fulfillment of the Requirements

For the Degree of

Master

in

Institute of Physics

June 2004

Hsinchu, Taiwan, Republic of China

Acknowledgments

Studying theoretical physics is an important decision for me. My parents played an important role in such a decision. Due to their support, I am able to make up my mind without hesitation. I like to dedicate this thesis to them.

I thank my advisors, Prof. Athar Husain and Prof. Guey-Lin Lin for their patience. During my first year in graduate school, Professor Guey-Lin Lin taught me the right attitude and essential physics needed to work on this thesis. He also provided an opportunity for me to do the thesis work with Prof. Athar Husain. I am grateful to Prof. Athar Husain for his kind guidance with great patience on my numerous mistakes. Step by step, he helped me to overcome various difficulties in this work.

Finally, I thank my girl friend, Yi-Chuen, for her encouragement during my difficult time. I like to share with her my pleasure of finishing up this thesis.

Abstract

The solar neutrino puzzle consists in observing a lower than expected solar electron neutrino flux by all solar neutrino detectors on earth. We study a particle physics solution to solve this puzzle. This solution assumes that the solar electron neutrinos oscillate into muon neutrinos during their journey to earth and thus remain unobserved. After briefly reviewing the essential standard solar model, the neutrino flavor oscillation probability in vacuum and in matter (the MSW effect including its Landau-Zener correction) is examined in some detail. Using these probability expressions, the solar electron neutrino event rates for various detectors are calculated and are compared with various observations including the day-night effect for solar neutrinos. A good agreement between them is found.

Key words: Standard Solar Model, Solar neutrino puzzle, Neutrino oscillations

Contents

Chapter 1

Introduction

The observed solar electron neutrino flux is different from what the theory predicts, this problem is commonly referred to as the Solar Neutrino Puzzle. In this thesis, we discuss the neutrino oscillations to solve the solar neutrino puzzle.

In 1930, Wolfgang Pauli postulated to the existence of a light neutral fermion, which he then called the *neutrone* to describe the continuous spectra of β-decay process. In modern terminology, the fundamental beta-decay process is: neutron goes to proton plus electron plus anti-neutrino

$$n \rightarrow p + e^- + \bar{\nu}. \tag{1.1}$$

After the advent of standard model of particle physics, the above process became

$$n \rightarrow p + e^- + \bar{\nu_e}. \tag{1.2}$$

The interaction between the neutrino and matter is extreme weakly, so the direct neutrino detection was difficult. In 1956, Cowan and Reines set up a large tank of water and watched for the *inverse* beta-decay reaction

$$\bar{\nu_e} + p \rightarrow n + e^+, \tag{1.3}$$

thus discovering $\bar{\nu}_e$. In 1962, Lederman, Schwartz, Steinberger and their collaborators found the second type of neutrino, ν_μ [1, 2].

This thesis is organized as follows: In chapter 1, we provide basic standard solar model knowledge. In chapter 2, we present the neutrino oscillation description with the vacuum condition and the survival probabilities are obtain from them by integration of the evolution equation. In chapter 3, we

consider more realistic condition. We rewrite the evolution equation for neutrino propagation and the survival probability in matter. In chapter 4, we calculate the ratio of solar electron neutrino event rates predicted in the neutrino oscillation scenario to the standard solar model event rate for the Ga and the Super-Kamiokande (SKK) experiments. Finally, in chapter 5, it is the summary and conclusion for this thesis.

1.1 Standard Solar Model

To investigate the puzzle of solar neutrinos, we must mention solar model first. Neutrinos are produced by core of sun, then pass through the whole mantle to arrive at surface. In such a process the solar influence on neutrinos could not be neglected. Thus, solar model is very important for studying the solar neutrino problem[3].

In 1939, a *Standard Solar Model* by Bethe detailed the formulation of the nuclear reaction cycles. A recent prediction is given by J. Bahcall and his collaboration. The "Standard Solar Model" is result of best physics input parameters that are available at the time the model is constructed. The set of numbers that correspond to the Standard Solar Model vary with time hopefully always getting closer to the true Standard Solar Model.

Here, we should emphasize that it would be impossible to summarize them in this thesis. We concentrate specifically on Bahcall-Pinsonneault 2004 (BP04) version of the standard solar model and call it SSM. We list the essential relevant parameters such as the electron number density profile and the neutrino energy spectrum in this model in next two subsection.

1.1.1 Properties of the Sun

The sun is a very useful astronomical laboratory. Because it is so close to earth, so that we can obtain information from the light which is being emitting from sun. From this information, we can determine precise values for solar mass, radius, geometric shape, photon spectrum, total luminosity, surface chemical composition and age.

From the photon spectrum, we can know the composition of sun. Because every element has it's own unique eigen spectrum. The experimental results tell us that it is mostly composition is hydrogen, second is helium. The solar energy is provided by nuclear reaction which we discuss in next subsection.

Table 1.1 summarizes some of these properties. The principal assumptions

Parameter	Value
Luminosity	3.86×10^{33}erg/s
Baryon number	$\sim 10^{57}$
Radius($R_\odot$)	6.96×10^{10} cm
Surface Temperature	5.78×10^{3} K
Core Temperature	1.56×10^{7} K
Age	$\approx 4.55 \times 10^{7}$ yr
Core density	148 g/cm^3
Depth of convective zone	$0.26R_\odot$

Table 1.1: Some important solar quantities[3].

that go into the calculation of these parameters are the following:

- Hydrostatic equilibrium of sun.
- Energy transport by photons.
- Energy generation by nuclear fusion.
- Relative abundance of different elements that is determined solely by nuclear reaction.

Additionally, we should refer to electron number density of sun. Because the electron number density distribution plays an important role in the dynamics of neutrino propagation inside the sun, as it's value depend on solar radius. The electron number density is calculated in standard solar model, the logarithm of the electron density divided by Avogadro's number can be approximated by the expression[3]

$$\log(n_e/N_A) = 2.32 - 4.17x - 0.000125/[x^2 + (0.5)^2], \tag{1.4}$$

where $x = R/R_\odot < 0.25$ and $N_A = 6.02 \times 10^{23}$ is the Avogadro's number. The unit of n_e is cm^{-3}. For the range between $0.25 \leq x \leq 0.75$, the equation for electron number density is

$$n_e/N_A = 245e^{-10.54x}. \tag{1.5}$$

In this thesis, we take the location of core at $0.1R_\odot$ where $R_\odot \simeq 6.96 \times 10^8$ m.

1.1.2 Solar Neutrino Flux Spectrum

In subsection (1.1.1), we have tabulated several parameters for sun. Another most important for our study is the solar neutrinos source and their propagation behavior inside the sun.

Sun is a huge fusion reactor. Hydrogen transforms into helium accompanying energy and neutrinos. In which the neutrino luminosity is 2.3% of the total photon luminosity.

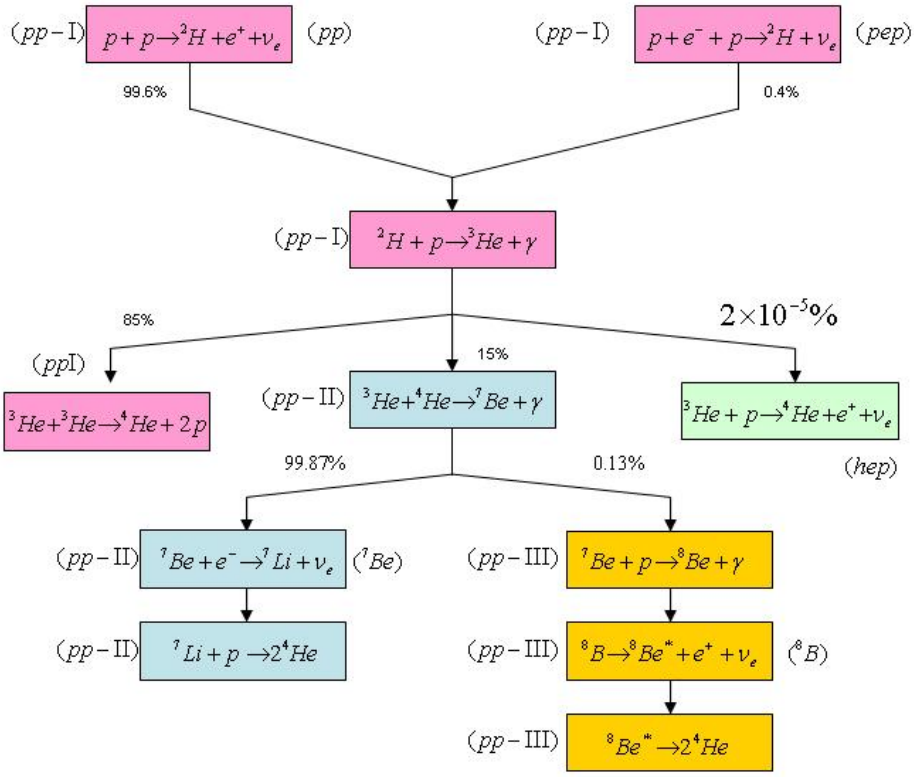

Figure 1.1: The solar *pp* cycle. The percentage means the fraction of contribution. We label the type of process at right side near the box.

There are two main cycles that occur in the sun, they are the pp cycle and the CNO cycle. In Fig. (1.1), the ν_e sources of pp cycle are shown. These are *pp*, *pep*, ^7Be, ^8B and *hep*. The two most important contribution

of ν_e fluxes are the pp flux with an *average* neutrino energy of 0.267 MeV and the ^7Be line with energy 0.863 MeV. The net reaction for pp cycle in the sun is given by

$$4p + 2e^- \quad \rightarrow \quad {}^4He + 2\nu_e + 26.73 \text{ MeV}. \tag{1.6}$$

In Fig. 1.1, the main branches to produce ^4He go via $^3He + ^3He$ and $^3He + ^4He$. The first one, has a probability 85% and the second one is 15%. Note that ^8B neutrinos have higher energy but they are much rarer. The CNO cycle is a small contribution for electron neutrino sources, it is about 1.6% of energy. CNO cycle dominates over the pp chain only if the temperature exceeds 1.8×10^7 K. For the sun, this condition is not met[4, 5]. In this thesis, we don't consider the CNO cycle contribution.

Experiment	ν_e-detection method	E^{th}/MeV	Main source
GALLEX	$\nu_e + {}^{71}\text{Ga} \rightarrow e^- + {}^{71}\text{Ge}$	0.233	pp,^{7}Be,^{8}B
SKK	$\nu_e + e^- \rightarrow \nu_e + e^-$	4.74	^{8}B
SNO	$\nu_e + e^- \rightarrow \nu_e + e^-$	5.24	^{8}B
	$\nu_e + d \rightarrow e^- + p + p$	6.4	
	$\nu_{\mu,e} + d \rightarrow \nu_{\mu,e} + p + n$	6.25	

Table 1.2: Some important experiments description that are used in this thesis. E^{th} is the threshold energy in MeV.

The *pp* cycle can be fractionized in three type, and we call them be $pp-I$ (85%), $pp-II$ (15%) and $pp-III$ (1.95×10^{-4}). According to Fig. 1.2, the pp process maximum energy is 0.42 MeV, pep is 1.44 MeV, hep is 18.77 MeV, ^{7}Be is 0.861 and ^{8}B is 14.06 MeV. Table 1.2 summarizes the main solar electron neutrino sources including the brief description of experiments, we consider in this thesis.

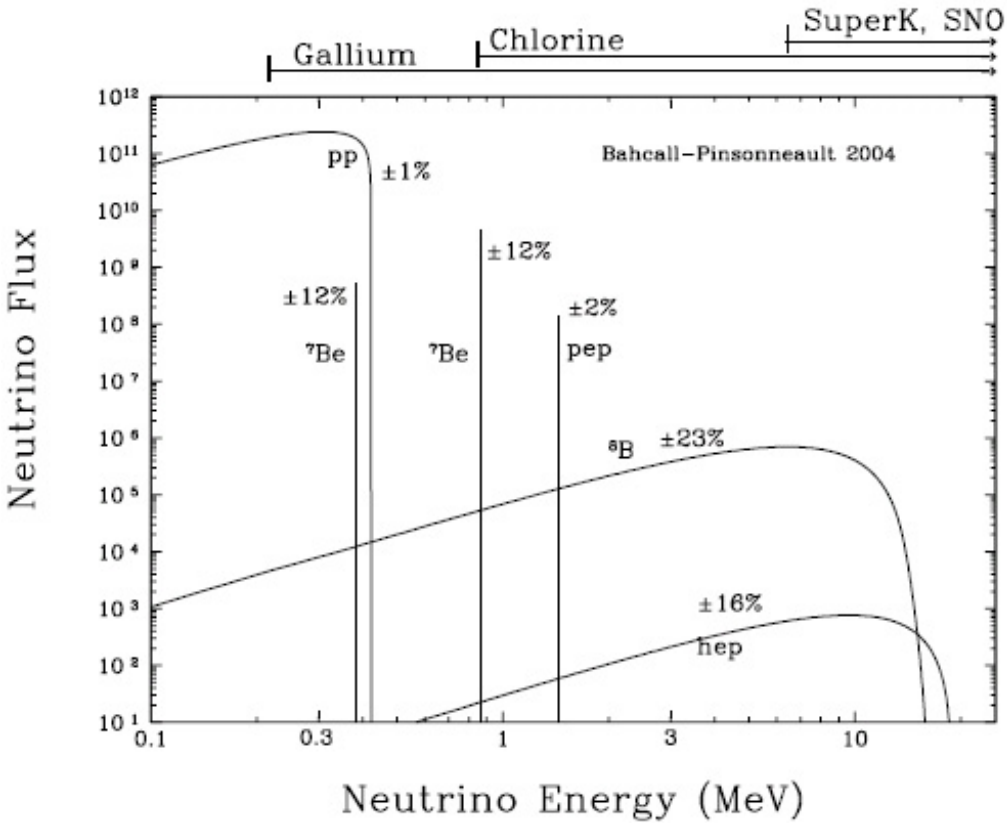

Figure 1.2: Energy spectra of neutrino fluxes from the *pp* chain, as predicted by the BP04 standard solar model. For continuous sources, the differential flux is in $\mathrm{cm}^{-2}\mathrm{s}^{-1}$ MeV^{-1}. For lines, the flux is in $\mathrm{cm}^{-2}\mathrm{s}^{-1}$. The percentage errors are the calculated 1σ uncertainties in predicted fluxes. The arrows at the top of the figure indicate the energy threshold for the various neutrino experiments.

Chapter 2

Neutrino Oscillation In Vacuum

2.1 Schrödinger Equation For Neutrino Propagation

Neutrinos may have either a Dirac or a Majorana mass, but for propagation of ultra-relativistic neutrinos the full spin structure is not probed. The weak interactions couple only to the *left-handed* component of the neutrino state. For neutrino with $p \gg m$, we shall deal the neutrino as *ultra-relativistic* neutrino for which the spin-structure is not revealed anyway[6].

The equation of motion in mass eigenstate basis is given by

$$(p^2 + m^2)|\nu\rangle = E^2|\nu\rangle. \tag{2.1}$$

Eq. (2.1) has two solution corresponding to waves traveling in opposite direction. However, the reflected solution shall not be relevant. Thus we throw away the reflected solution to get

$$E = \sqrt{p^2 + m^2}. \tag{2.2}$$

In the first-order approximation for $p \gg m$, we obtain

$$E \simeq p + \frac{m^2}{2p}. \tag{2.3}$$

Using the substitution $-i\frac{\partial}{\partial x} \to p$, $i\frac{\partial}{\partial t} \to E$ and $p \simeq E$,we obtain

$$i\frac{\partial}{\partial t}|\nu\rangle = (E + \frac{m^2}{2E})|\nu\rangle = H|\nu\rangle. \tag{2.4}$$

This equation describes the propagation of an ultra-relativistic neutrino. There H is diagonal in this basis and is given by

$$H = \begin{pmatrix} E_1 & 0 \\ 0 & E_2 \end{pmatrix} \simeq E + \begin{pmatrix} \frac{m_1^2}{2E} & 0 \\ 0 & \frac{m_2^2}{2E} \end{pmatrix}. \tag{2.5}$$

The plan-wave solution of Eq. (2.4) in usual notation is

$$\nu(x,t) = e^{-i\int H dt}\nu(x,0). \tag{2.6}$$

Next, we examine the survival probability using this information.

2.2 The Survival Probability In Vacuum

If the mass eigenstates are not the same as the weak-interaction eigenstates, then the neutrino mixing will occur. This behavior is so-called *neutrinos oscillation*. In other words, the neutrinos oscillation means that the neutrino flavour change from one flavour to the other flavour. We aim to discuss the survival probability below.

Consider the relation of linear combination between weak-interaction eigenstates and mass eigenstates for two flavours as

$$\begin{pmatrix} \nu_e \\ \nu_\mu \end{pmatrix} = U \begin{pmatrix} \nu_1 \\ \nu_2 \end{pmatrix}. \tag{2.7}$$

Where ν_e and ν_μ are weak-interaction eigenstates, and ν_1 and ν_2 are mass eigenstates. U a 2×2 unitary matrix and is given by

$$U \equiv \begin{pmatrix} C_\theta & S_\theta \\ -S_\theta & C_\theta \end{pmatrix}, \tag{2.8}$$

here C_θ denote by $\cos\theta$ and S_θ denote by $\sin\theta$. The θ we call it be vacuum mixing angle and we can choose $0 \leq \theta \leq \frac{\pi}{4}$.

The solution (2.6) for the neutrino wave function can be rewritten for two neutrino species as

$$\begin{pmatrix} \nu_1(t) \\ \nu_2(t) \end{pmatrix} = \begin{pmatrix} e^{-iE_1 t} & 0 \\ 0 & e^{-iE_2 t} \end{pmatrix} \begin{pmatrix} \nu_1(0) \\ \nu_2(0) \end{pmatrix}. \tag{2.9}$$

If we produce an electron neutrino, the probability of detecting this neutrino as an electron after a time t, can be written as

$$P(\nu_e \to \nu_e) = |\langle \nu_e(t) \mid \nu_e(0) \rangle|^2 ,$$

$$= \left| \begin{pmatrix} 1 & 0 \end{pmatrix} \begin{pmatrix} C_\theta & S_\theta \\ -S_\theta & C_\theta \end{pmatrix} \begin{pmatrix} e^{-iE_1 t} & 0 \\ 0 & e^{-iE_2 t} \end{pmatrix} \begin{pmatrix} C_\theta & -S_\theta \\ S_\theta & C_\theta \end{pmatrix} \begin{pmatrix} 1 \\ 0 \end{pmatrix} \right|^2 . \quad (2.10)$$

From matrix form (2.10) we get the concise formula of survival probability as follows

$$P(\nu_e \to \nu_e) = 1 - \frac{1}{2} \sin^2 2\theta [1 - \cos(E_2 - E_1)t], \quad (2.11)$$

where $E_2 - E_1$ approach to $(m_2^2 - m_1^2)/2E$, using Eq. (2.5). Hereafter, we shall use the symbol δm^2 instead of $(m_2^2 - m_1^2)$ and λ instead of $4\pi E/\delta m^2$ and call it the *oscillation length* λ, which can show below in numerical form. It is given by

$$\lambda = 2.48\,\mathrm{m} \times \left(\frac{\mathrm{E}}{\mathrm{MeV}} \right) \left(\frac{\mathrm{eV}^2}{\delta \mathrm{m}^2} \right) . \quad (2.12)$$

Using these notations Eq. (2.11) becomes

$$P(\nu_e \to \nu_e) = 1 - \sin^2 2\theta \sin^2 \left(\frac{\pi}{\lambda} x \right) , \quad (2.13)$$

here x is propagation distance. If propagation distance equal to oscillation length or mixing angle equal to zero, then we can find oscillation almost disappear. Oppositely, when $\theta = \frac{\pi}{4}$ and $x \sim \frac{\lambda}{2}$ the oscillation is maximum. For example, if neutrinos energy about 10^3 MeV and $\delta m^2 = 10^{-5}\mathrm{eV}^2$ then λ equal to 2.48×10^8 m. In other words, λ is about radius of earth.

In the next section we shall figure out the behavior of λ, δm^2 and survival probability in light of data of Super-Kamiokande detector.

If the production or detection positions extend over a distance much larger than the wavelength, the phase information shall be averaged out. If the phase information is lost, then the probability is just the classical probability. The phase acquired during neutrino propagation is averaged out; so we can sum incoherently over the propagation eigenstates, the mass eigenstates:

$$P(\nu_e \to \nu_e) = \sum_{i=1,2} P(\nu_e \to \nu_i) P(\nu_i \to \nu_e), \quad (2.14)$$

$$= \left| \begin{pmatrix} 1 & 0 \end{pmatrix} \begin{pmatrix} C_\theta^2 & S_\theta^2 \\ S_\theta^2 & C_\theta^2 \end{pmatrix} \begin{pmatrix} 1 & 0 \\ 0 & 1 \end{pmatrix} \begin{pmatrix} C_\theta^2 & S_\theta^2 \\ S_\theta^2 & C_\theta^2 \end{pmatrix} \begin{pmatrix} 1 \\ 0 \end{pmatrix} \right|. \tag{2.15}$$

After average out of phase, then

$$P(\nu_e \to \nu_e) = 1 - \frac{1}{2}\sin^2 2\theta. \tag{2.16}$$

2.3 Vacuum Oscillation For Solar Neutrinos

In Section 2.1 and 2.2, we discussed the vacuum oscillations qualitatively. Here, we have interest in applying the result to solve the solar neutrino problem in quantitative terms.

Neutrino was produced inside the sun, then it propagated from sun to earth. Finally, the neutrino was detected by detector. This process of propagation has a long distance between sun surface and earth surface in vacuum. In this section, we shall try to know how to explain the range of δm^2 and $\sin^2 2\theta$ to explain the Super-Kamiokande observation of ^8B flux in comparison with standard solar model ^8B flux.

In standard model BP04[5], the ^8B flux is

$$\Phi^{SM} = 5.79(1 \pm 0.23) \times 10^6 \text{ cm}^{-2}\text{s}^{-1}. \tag{2.17}$$

And the flux detected by Super-Kamiokande[7] and SNO[8] respectively are

$$\begin{aligned} \Phi_D^{SKK} &= (2.32 \pm 0.03) \times 10^6 \text{ cm}^{-2}\text{s}^{-1}, \\ \Phi_D^{SNO} &= (1.76 \pm^{0.06}_{0.05} \pm 0.09) \times 10^6 \text{ cm}^{-2}\text{s}^{-1}. \end{aligned} \tag{2.18}$$

If we follow standard model prediction and don't consider the Oscillation effect we get the Φ^{SM}. The Φ_D^{SKK} tokes into account the elastic ($\nu_e e \to \nu_e e$) scattering. The Φ_D^{SNO} takes into account the change current scattering also in $\nu_e + d \to e^- + p + p$ (see Table 1.2 also). But, in fact the experiment reminds us that indeed this is not the case. If we add the vacuum oscillation so that the ratio of flux is equal to oscillation probability using Eq. (2.13), we can then use the ratio to fix the probability.

$$\Phi_D^{exp} = P(\nu_e \to \nu_e)\Phi^{SM}. \tag{2.19}$$

In Fig. 2.1, below the curve is non-allowed region, as the neutrino energy is smaller than threshold energy. So, in this situation, we get the following

range of δm^2 and $\sin^2 2\theta$ for SKK is

$$\begin{aligned} 2.23 \times 10^{-11} &\leq \delta m^2/\mathrm{eV}^2 \leq 3.85 \times 10^{-11}, \\ 0.6 &\leq \sin^2 2\theta \leq 1. \end{aligned} \tag{2.20}$$

We also obtain the result for SNO as follows

$$\begin{aligned} 3.34 \times 10^{-11} &\leq \delta m^2/\mathrm{eV}^2 \leq 5.24 \times 10^{-11}, \\ 0.70 &\leq \sin^2 2\theta \leq 1. \end{aligned} \tag{2.21}$$

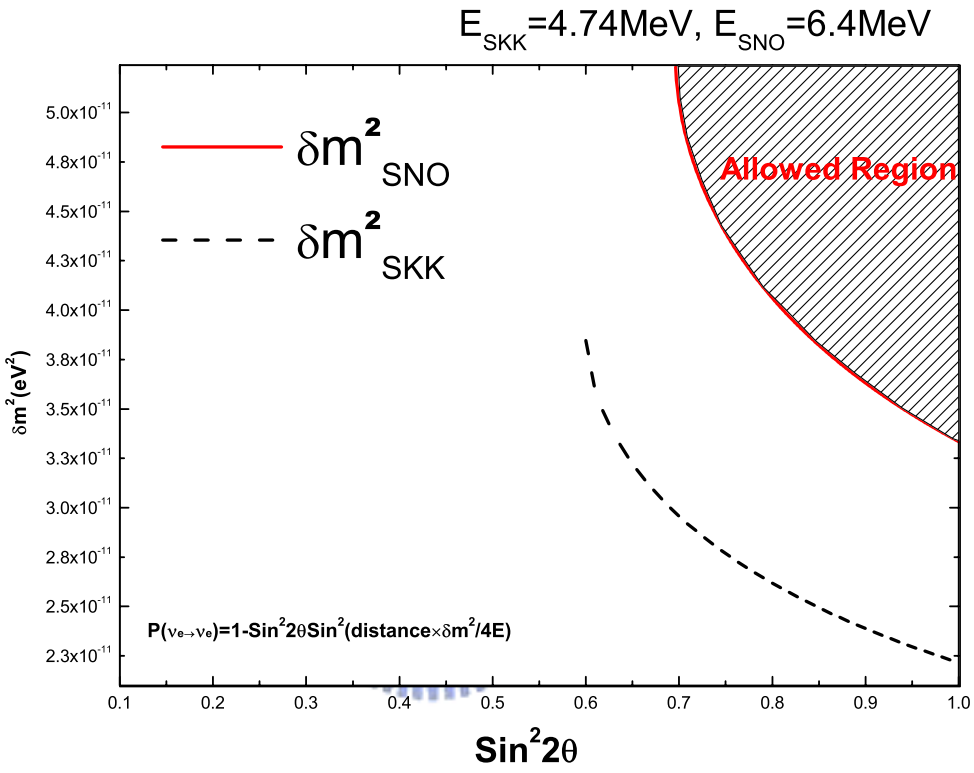

Figure 2.1: The figure consider vacuum oscillations only. We fix the value of probability as 0.40 for SKK and 0.30 for SNO, see Eq. (2.19). The distance between earth and sun is about 1.5×10^{13} cm. The threshold energy of SKK is 4.74 MeV and SNO is 6.4 MeV.

Chapter 3

Neutrino Oscillation In Matter

To analyze the propagation of solar neutrinos, we can separate three components of process. First one is neutrino produced inside the core of sun then pass through the mantle arriving at the surface. Second is from sun surface to earth surface, which is what we discuss in preceding chapter. Last component is passage through that whole earth. In which, first part and third part must consider the effect of neutrinos interaction with matter. Solving the wave equation analytically is difficult so that we need an approximation method. Mikheyev, Smirnov and Wolfenstein (MSW) developed an approximation method to avoid solving wave function directly. In this chapter, we shall pay our attention to use MSW method for solving solar neutrinos problem.

3.1 Schrödinger Equation For Neutrino Propagation in Matter

When neutrinos propagate through matter ν_e and ν_μ feel different potentials, because ν_e scatters off electron via both neutral and charge currents, whereas ν_μ scatters only via the neutral current (see Fig. 3.1). There are two types of weak interactions, the charge current interaction, which is mediated by the exchange of $W^\pm$ gauge bosons, and the neutral current interaction, which is mediated by the exchange of Z gauge bosons.

The neutral current contribution is the same for all flavours of neutrinos, whereas the charge current contribution affect ν_e only. The contribution of charge current for neutrino propagation is contained in the parameter A,

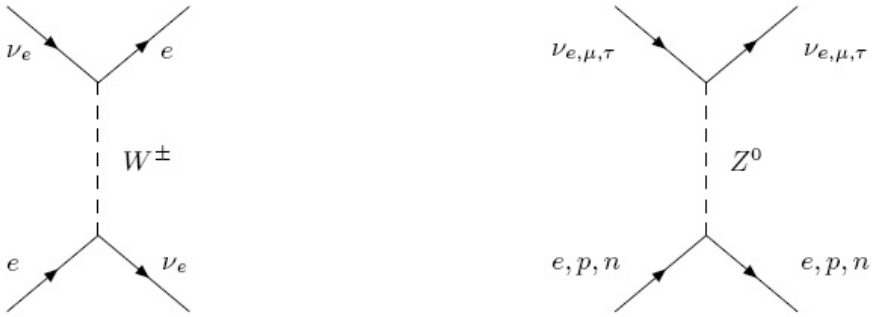

Figure 3.1: Feynman diagrams for charge current and neutral current exchange.

given by

$$A \equiv 2\sqrt{2}G_F N_e E = 2\sqrt{2}G_F \frac{Y_e}{m_n}\rho E, \tag{3.1}$$

where G_F is Fermi-constant, ρ the density, Y_e the number of electrons per nucleon, and m_n the nucleon mass. A is potential for charge current in the so-called nature units. The neutrino propagation Eq. (2.4) with $c = 1$, $t \to x$ in weak-interaction eigenstate basis and neglecting non-important constant term, can be rewritten as

$$i\frac{\partial}{\partial x}\begin{pmatrix} \nu_e \\ \nu_\mu \end{pmatrix} = \frac{1}{2E}\left[U\begin{pmatrix} m_1^2 & 0 \\ 0 & m_2^2 \end{pmatrix}U^\dagger + \begin{pmatrix} A & 0 \\ 0 & 0 \end{pmatrix}\right]\begin{pmatrix} \nu_e \\ \nu_\mu \end{pmatrix}. \tag{3.2}$$

Let us to write down the eigenvalue of the Hamiltonian as

$$\lambda_\pm = \{(m_1^2 + m_2^2 + A) \pm \sqrt{[(A - \delta m^2 C_{2\theta})^2 + (\delta m^2 S_{2\theta})^2]}\}/4E. \tag{3.3}$$

To mimic the situation of the vacuum for convenience, we should have new parameter for mixing-matrix and mass-matrix in medium. The mass-matrix is

$$\begin{aligned} M &= \begin{pmatrix} M_1^2 & 0 \\ 0 & M_2^2 \end{pmatrix}, \\ M_{2,1}^2 &= \{(m_1^2 + m_2^2 + A) \pm \sqrt{[(A - \delta m^2 C_{2\theta})^2 + (\delta m^2 S_{2\theta})^2]}\}/2. \end{aligned} \tag{3.4}$$

M can be diagonalized by mixing-matrix, it's similar to Eq. (2.7) and (2.8),

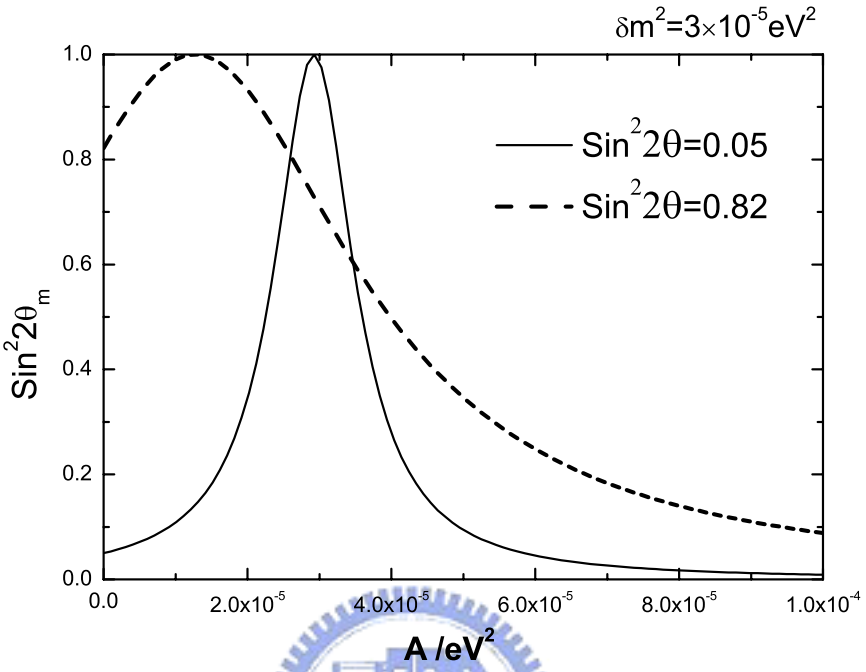

Figure 3.2: Plot of $\sin^2 2\theta_m$ as function of A for two different value of θ. The θ_m is the effective neutrino mixing angle in matter. The large mixing angle corresponds to 32.5^o.

and is given by

$$\begin{pmatrix} \nu_e \\ \nu_\mu \end{pmatrix} = U^m \begin{pmatrix} \nu_1^m \\ \nu_2^m \end{pmatrix} = \begin{pmatrix} C_{\theta_m} & S_{\theta_m} \\ -S_{\theta_m} & C_{\theta_m} \end{pmatrix} \begin{pmatrix} \nu_1^m \\ \nu_2^m \end{pmatrix}. \tag{3.5}$$

The mass eigenstates in the medium are $|\nu_1^m\rangle$ and $|\nu_2^m\rangle$. Here θ_m is the neutrino mixing angle in matter. From Eq. (3.5), we can see that the diagonalizing angle[1] is given by

$$\cos 2\theta_m = \frac{-A + \delta m^2 C_{2\theta}}{\sqrt{[(A - \delta m^2 C_{2\theta})^2 + (\delta m^2 S_{2\theta})^2]}},$$

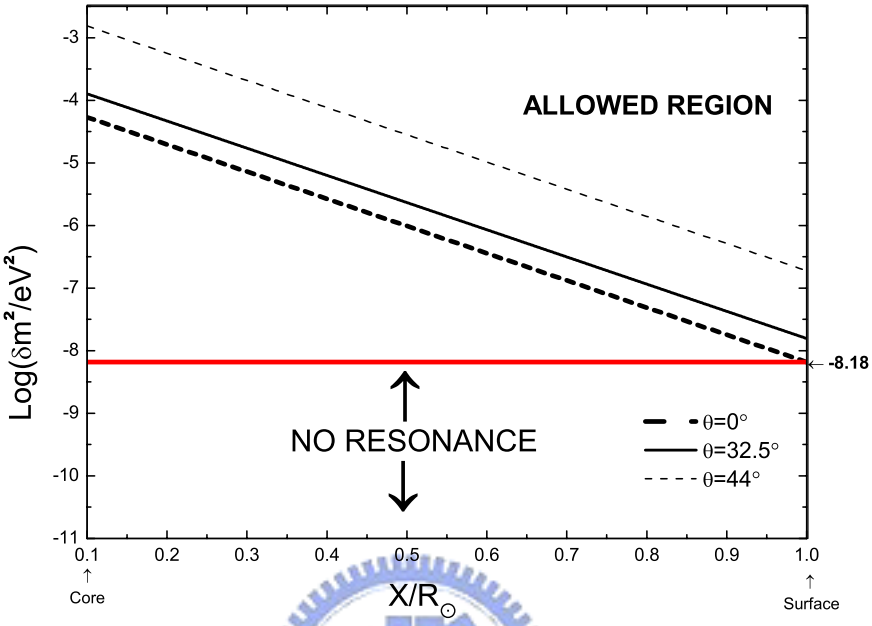

Figure 3.3: The result of combining Eq. (1.5), (3.1) and (3.7). We take the energy of neutrino as 4.74 MeV. When $\log(\delta m^2/\mathrm{eV}^2)$ is less then -8.18, there is no resonance inside Sun.

$$\sin 2\theta_m = \frac{\delta m^2 S_{2\theta}}{\sqrt{[(A-\delta m^2 C_{2\theta})^2 + (\delta m^2 S_{2\theta})^2]}}. \tag{3.6}$$

We find the mixing angle is modified substantially by the coherent scattering of a medium, as show in Fig. 3.2.

In Fig. 3.2, we are interested in the following three main limits for A, $A \to 0$, $A \to \infty$ and $A = \delta m^2 C_{2\theta}$. When $A \to 0$, that means neutrinos propagate in vacuum, so that the mixing matrix is just the vacuum expression. When $A \to \infty$, we obtain, $\theta_m \to \frac{\pi}{2}$. When $A = \delta m^2 C_{2\theta}$, we can see a peak value in $\sin^2 2\theta_m$ which is so-called resonance. So, the resonance condition is given by

$$A = \delta m^2 C_{2\theta}. \tag{3.7}$$

In resonance, as $\sin^2 2\theta_m$ is maximum and thus, it can enhance neutrino oscillations maximally. In Eq. (3.7), we find the resonance occurs essentially irrespective of whether or not the mixing angle is small. The resonance would not occur if θ is greater as then $\frac{\pi}{4}$. In that case the resonance would occur for anti-neutrinos. Since for anti-neutrinos the resonance condition must be changed by the substitution A to $-A$. Eq. (3.1) shows that A is function of electron number density. The density of sun is give by Eq. (1.5).

Applying the Eq. (1.5) into resonance condition, then we can find the range where is resonance (Fig. 3.3). The figure tells us when $\delta m^2/\mathrm{eV}^2$ small then $10^{-8.18}$ there is no resonance region inside the sun. According to this result, we can check the range of vacuum oscillation for Eq. (2.20). The vacuum oscillation range is between 3.85×10^{-11} eV^2 and 2.61×10^{-11} eV^2 which is outside the prediction of Fig. 3.3.

If we assume $\delta m^2/\mathrm{eV}^2$ is set inside the range and we can use the same condition as Fig. (3.2). Here, we just consider one particle is produced in core and carry 5 MeV energy to propagate. When it travels from core to surface, the $\sin^2 2\theta_m$ is changed with the radius and the resonance position is about $0.26R_\odot$ under this condition.

3.2 The MSW Effect

In section 3.1, we discussed the Schrödinger Equation in matter and where the resonance region is. Let us now examine the experimentally observable quantity $P(\nu_e \to \nu_e)$, which is the probability for a produced ν_e to remain a ν_e after propagation.

Eq. (2.9) is time-evolution for mass-eigenstate propagating in vacuum. For neutrinos propagating in matter, the Eq. (2.9) needs to be modified. Indeed, we may write the neutrinos propagation Eq. (3.2) in the form

$$i\frac{\partial}{\partial x}\left[U^m \begin{pmatrix} \nu_1 \\ \nu_2 \end{pmatrix}\right] = \frac{1}{2E}\left[U^m \begin{pmatrix} M_1^2 & 0 \\ 0 & M_2^2 \end{pmatrix} U^{m\dagger}\right] U^m \begin{pmatrix} \nu_1 \\ \nu_2 \end{pmatrix}. \tag{3.8}$$

Here, neutrinos are propagating in matter, the density change is in x, so that U^m depends on x. Then, we may rewrite Eq. (3.8) as

$$i\frac{\partial}{\partial x}\begin{pmatrix} \nu_1 \\ \nu_2 \end{pmatrix} = \begin{pmatrix} \frac{M_1^2}{2E} & -i\frac{\partial}{\partial x}\theta_m \\ i\frac{\partial}{\partial x}\theta_m & \frac{M_2^2}{2E} \end{pmatrix}\begin{pmatrix} \nu_1 \\ \nu_2 \end{pmatrix}. \tag{3.9}$$

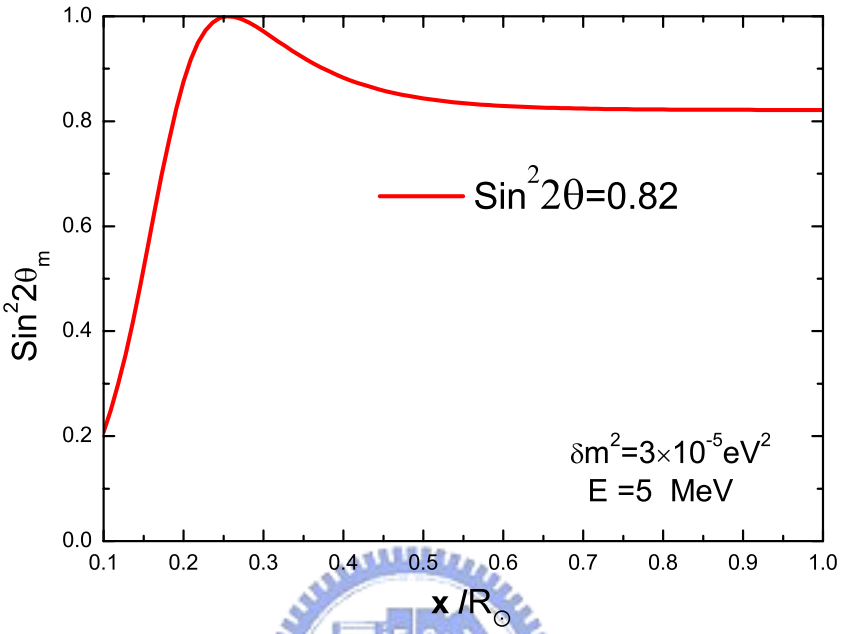

Figure 3.4: This figure describes the resonance position inside the sun. The peak value is about x = $0.26R_\odot$ and the mixing angle we take $\theta = 32.5^o$.

We can always take out a common diagonal phase factor so that Eq. (3.9) become

$$i\frac{\partial}{\partial x}\begin{pmatrix}\nu_1'\\ \nu_2'\end{pmatrix} = \begin{pmatrix}-\frac{M_2^2-M_1^2}{4E} & -i\frac{\partial}{\partial x}\theta_m\\ i\frac{\partial}{\partial x}\theta_m & \frac{M_2^2-M_1^2}{4E}\end{pmatrix}\begin{pmatrix}\nu_1'\\ \nu_2'\end{pmatrix}. \tag{3.10}$$

The diagonal phase factor is

$$\begin{pmatrix}\nu_1\\ \nu_2\end{pmatrix} = \begin{pmatrix}e^{-a} & 0\\ 0 & e^{-a}\end{pmatrix}\begin{pmatrix}\nu_1'\\ \nu_2'\end{pmatrix}, \tag{3.11}$$

where the a is phase factor given by

$$a = i\frac{M_2^2+M_1^2}{4E}x.$$

For the case of solar neutrinos, the oscillation distance is large enough. Therefore, the phase factor was dropped during the derivation of the wave equation. But, how to solve Eq. (3.10)? It's difficult to get the exact solution. Mikheyev, Smirnov and Wolfenstein assume the condition $\frac{M_2^2-M_1^2}{4E} \gg i\frac{\partial\theta_m}{\partial x}$, then we can solve equation under this condition. This effect is so-call *MSW effect*, and the condition we call it be *adiabatic condition*. The MSW effect describes how matter can enhance the flavor oscillation of neutrinos[9, 10]. Using Eqs. (3.4) and (3.6) we have

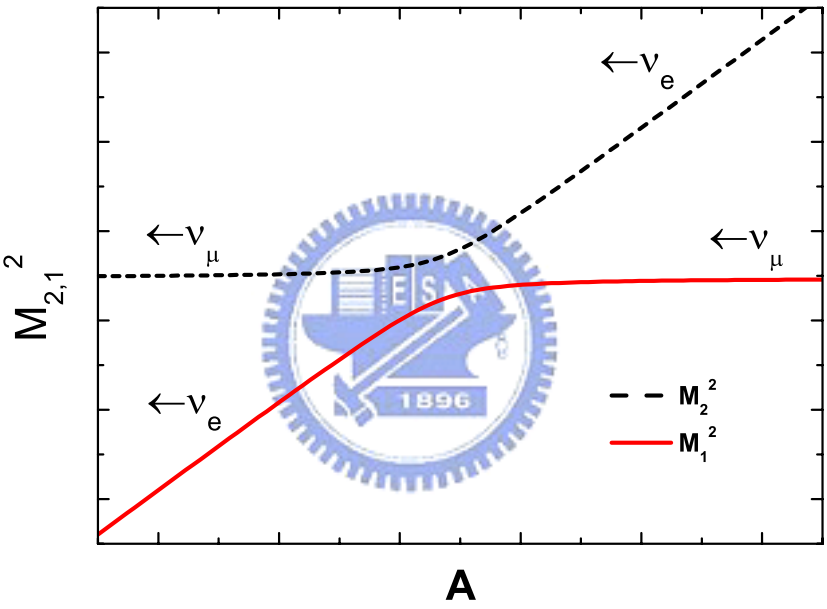

Figure 3.5: Schematic diagram for the effective neutrino mass squared of two flavors of neutrinos as function of A. Here we take $m_2^2 = 25m_1^2$, $\sin^2 2\theta = 1 \times 10^{-2}$. More details are given in the text.

$$(M_2^2 - M_1^2) = \sqrt{[(A - \delta m^2 C_{2\theta})^2 + (\delta m^2 S_{2\theta})^2]}, \tag{3.12}$$

$$\frac{\partial\theta_m}{\partial x} = \frac{1}{2}\frac{\delta m^2 S_{2\theta}}{(A - \delta m^2 C_{2\theta})^2 + (\delta m^2 S_{2\theta})^2}\frac{\partial A}{\partial x}. \tag{3.13}$$

Substituting Eq. (3.12) and Eq. (3.13) back in adiabatic condition, we obtain

$$\frac{1}{2E}\frac{[(A-\delta m^2 C_{2\theta})^2+(\delta m^2 S_{2\theta})^2]^{3/2}}{A\delta m^2 S_{2\theta}} \gg \frac{1}{n_e}\frac{dn_e}{dx}. \tag{3.14}$$

This inequality is very useful for next section, here we just keep this form. According to inequality (3.14), the density changes slowly enough so that the propagation is adiabatic. Then we should pay our attention in Eq. (3.12). Because M_2^2 and M_1^2 are eigenvalues of neutrinos flavor eigenstate. Now, they vary with A as can be seen form Fig. 3.5. The flavor eigenstate $|\nu_e\rangle$ is created at larger A in solar interior where it is approximately the same as the heavier mass eigenstate $|\nu_2\rangle$. As the electron density decreases slowly, the flavor remains close to the mass eigenstate $|\nu_2\rangle$. The probabilities of ν_e to either ν_1 or ν_2 are given by $\sin^2\theta_m$ and $\cos^2\theta_m$, respectively. Let us assume that, after production, a ν_e propagates adiabatically until reaching a location for which electron density equal to zero and the mixing angle is the vacuum angle. The probability of ν_1 or ν_2 to be a ν_e is then given by $\sin^2\theta$ and $\cos^2\theta$, respectively.

Now, we consider the evolution equation again in the following form

$$\begin{pmatrix} \nu_1(x) \\ \nu_2(x) \end{pmatrix} = \begin{pmatrix} e^{-\frac{\delta M^2}{4E}x} & 0 \\ 0 & e^{\frac{\delta M^2}{4E}x} \end{pmatrix} \begin{pmatrix} \nu_1(0) \\ \nu_2(0) \end{pmatrix}, \tag{3.15}$$

here, we define the δM^2 as $M_2^2 - M_1^2$. Compared to Eq. (2.11), change is to replace δm^2 with δM^2. Using it, we can get the survival probability for constant density. At far distance, we can average out the phase term

$$P(\nu_e \to \nu_e) = 1 - \frac{1}{2}\sin^2 2\theta_m. \tag{3.16}$$

This is the generalization of Eq. (2.11) with the replacement $\theta \to \theta_m$.

For adiabatic condition, as the same result with Eq. (2.14), the survival probability for neutrinos propagation between vacuum and matter in the adiabatic approximation is

$$P(\nu_e \to \nu_e) = \sum_{i=1,2} P_m(\nu_e \to \nu_i) P(\nu_i \to \nu_e),$$

$$= \left| \begin{pmatrix} 1 & 0 \end{pmatrix} \begin{pmatrix} C_{\theta_m}^2 & S_{\theta_m}^2 \\ S_{\theta_m}^2 & C_{\theta_m}^2 \end{pmatrix} \begin{pmatrix} 1 & 0 \\ 0 & 1 \end{pmatrix} \begin{pmatrix} C_\theta^2 & S_\theta^2 \\ S_\theta^2 & C_\theta^2 \end{pmatrix} \begin{pmatrix} 1 \\ 0 \end{pmatrix} \right|. \tag{3.17}$$

Evaluating the matrix, we can get the probability as $\frac{1}{2}(1+\cos 2\theta \cos 2\theta_m)$.

In general, if an electron neutrino propagate adiabatically from one region with mixing-angle θ_1, to another region with mixing-angle θ_2, then

$$P(\nu_e \to \nu_e) = \frac{1}{2}(1+\cos 2\theta_1 \cos 2\theta_2). \tag{3.18}$$

3.3 Landau-Zener Probability

The MSW effect is valid only when the matter density changes slowly, so that the adiabatic approximation is valid. When MSW approximation breaks down, we must go back and solve the wave equation directly. We can see Eq. (3.13), $\frac{d\theta_m}{dx}$ has a sharply peaked maximum, and Eq. (3.12), $M_2^2 - M_1^2$ has a minimum in resonance. Therefore, we should check the validity of adiabatic condition.

Eq. (3.14) can be rewritten as

$$\frac{\delta m^2 S_{2\theta}^2}{2EC_{2\theta}} \gg \left|\frac{1}{n_e}\frac{dn_e}{dx}\right|_{res}. \tag{3.19}$$

The subscript *res* indicates that this quantity should be evaluated at the resonance. Here, we move the term $\left|\frac{1}{n_e}\frac{dn_e}{dx}\right|_{res}$ to left hand side and denotes all this by the γ called the adiabatic parameter, so that Eq. (3.19) become

$$\gamma \gg 1. \tag{3.20}$$

The γ is very important for discussion of Landau-Zener effect.

In preceding section, we have discussed the case of adiabatic condition, namely $\gamma \gg 1$. Now, if $\gamma \approx 1$, there shall be considerable corrections to the probabilities obtained using the adiabatic approximation.

Referring again to Fig.(3.5), the electron neutrinos produced in core passes through resonance region and then arrival to vacuum region. We can correct the Eq. (3.17) accordingly

$$P(\nu_e \to \nu_e) = \sum_{i,j=1,2} P_m(\nu_e \to \nu_i) P_{res}(\nu_i \to \nu_j) P(\nu_j \to \nu_e), \tag{3.21}$$

$$= \left| \begin{pmatrix} 1 & 0 \end{pmatrix} \begin{pmatrix} C_{\theta_m}^2 & S_{\theta_m}^2 \\ S_{\theta_m}^2 & C_{\theta_m}^2 \end{pmatrix} \begin{pmatrix} 1-P_{LZ} & P_{LZ} \\ P_{LZ} & 1-P_{LZ} \end{pmatrix} \begin{pmatrix} C_\theta^2 & S_\theta^2 \\ S_\theta^2 & C_\theta^2 \end{pmatrix} \begin{pmatrix} 1 \\ 0 \end{pmatrix} \right|. \tag{3.22}$$

We expand the above matrix after averaging, and get

$$P(\nu_e \to \nu_e) = \frac{1}{2} + (\frac{1}{2} - P_{LZ}) \cos 2\theta \cos 2\theta_m, \tag{3.23}$$

where the P_{LZ} is crossing resonance probability, and the definition is

$$P_{LZ} \equiv \left| \langle \nu_2(x_+) | \nu_1(x_-) \rangle \right|^2 . \tag{3.24}$$

Here, $x_\pm$ refer to two faraway points on either side of the resonance position.

Such a level-crossing solution was first worked out by Landau and Zener in 1932[11] . So, we also call it Landau-Zener probability. To briefly sketch its derivation, we start with a mixed system of two neutrinos in flavor basis ν_e and ν_μ, the Hamilitonian is given by Eq. (3.2)

$$H\Psi = \begin{pmatrix} \epsilon_1 & \epsilon_{12} \\ \epsilon_{12} & \epsilon_2 \end{pmatrix} \Psi, \tag{3.25}$$

here we ignore the constant term and take $\epsilon_1 = \sqrt{2} G_{\rm F} n_{\rm e}(t) - \left(\frac{\delta m^2}{4{\rm E}}\right) \cos 2\theta$, $\epsilon_2 = \frac{\delta m^2}{4{\rm E}} \cos 2\theta$ and $\epsilon_{12} = \frac{\delta m^2}{4{\rm E}} \sin 2\theta$. Let Ψ be such linear combination of an orthonormal basis (C_1, C_2), we can rewrite Ψ as

$$\Psi = \begin{pmatrix} C_1(t) e^{-i\int \epsilon_1 dt} \\ C_2(t) e^{-i\int \epsilon_2 dt} \end{pmatrix}. \tag{3.26}$$

We set resonance position at $t = 0$, the initial condition for $|C_1(-\infty)|^2 = 1$ and $|C_2(-\infty)|^2 = 0$. We can see in Fig. 3.5, C_1 has the characteristics which $|\nu_e\rangle$ has at $A \gg A_{res}$, while C_2 has the characteristics which $|\nu_\mu\rangle$ has at $A \ll A_{res}$. Then, the problem is to find the probability that Ψ jump from the upper to the lower branch in the resonance region. We emphasize here, these subscriptions 1,2 are opposite with Fig. 3.5. We just need to find $|C_1(+\infty)|^2 \equiv P_{LZ}$ (that is Landau-Zener probability).

The Schrödinger equation is written

$$\begin{pmatrix} \epsilon_1 & \epsilon_{12} \\ \epsilon_{12} & \epsilon_2 \end{pmatrix} \begin{pmatrix} C_1(t) e^{-i\int \epsilon_1 dt} \\ C_2(t) e^{-i\int \epsilon_2 dt} \end{pmatrix} = i \frac{d}{dt} \begin{pmatrix} C_1(t) e^{-i\int \epsilon_1 dt} \\ C_2(t) e^{-i\int \epsilon_2 dt} \end{pmatrix}. \tag{3.27}$$

We now eliminate $C_1(t)$ to get a relation for $C_2(t)$ only

$$\frac{d^2 C_2(t)}{dt^2} - i\,(\epsilon_2 - \epsilon_1) \frac{dC_2(t)}{dt} + \epsilon_{12}^2 C_2(t) = 0. \tag{3.28}$$

Let us recall the resonance condition,

$$\sqrt{2}G_{\rm F}n_{\rm e}^{res} = \left(\frac{\delta m^2}{2{\rm E}}\right)\cos 2\theta. \tag{3.29}$$

Using resonance condition, we note that $\epsilon_2 - \epsilon_1 = \sqrt{2}G_{\rm F}n_{\rm e}(t) - \left(\frac{\delta m^2}{2{\rm E}}\right)\cos 2\theta$. Here, we assume $n_{\rm e}(t)$ be linear function

$$n_{\rm e}(t) = n_{\rm e}^{res} + \frac{dn_{\rm e}^{res}}{dt}(t - x_{res}). \tag{3.30}$$

We introduce a new parameter α, $\alpha = \sqrt{2}G_{\rm F}\frac{dn_{\rm e}^{res}}{dt}$, and $\epsilon_2 - \epsilon_1 = \alpha t$ then we rewrite Eq. (3.28) by letting $C_2(t) = e^{\frac{-i}{2}\int \epsilon_2 - \epsilon_1 dt}U(t)$. We then obtain

$$\frac{d^2U(z)}{dz^2} + \left(n - \frac{z^2}{4} + \frac{1}{2}\right)U(z) = 0. \tag{3.31}$$

Eq. (3.31) is called it Weber Equation, with $z = \sqrt{\alpha}e^{-i\frac{\pi}{4}}t$ and $n = i\frac{\epsilon_{12}^2}{\alpha}$. The details of how to solve Eq. (3.31) are given in appendix A. Here we use the results obtained there.

The solution of Eq. (3.31) is $U(z) = A_+ D_{-n-1}(-iz)$, where A_+ is normalization factor and the value is equal to $\sqrt{\nu}e^{-\frac{\pi\nu}{4}}$ with $\nu = -in = \frac{\epsilon_{12}^2}{\alpha}$. Here we take $z = Re^{i\frac{\pi}{4}}$, and R is the real number as function of time. After substitute these parameters, we obtain

$$C_2(t) = e^{\frac{-i}{2}\int(\epsilon_2 - \epsilon_1)dt}A_+ D_{-n-1}(-iz), \tag{3.32}$$

Where

$$D_{-n-1}(iRe^{i\frac{3\pi}{4}}) \sim \frac{\sqrt{2\pi}}{\Gamma(n+1)}e^{-in\frac{\pi}{4}}e^{-i\frac{R^2}{4}}R^n + e^{i\frac{3(n+1)\pi}{4}}e^{-i\frac{R^2}{4}}R^{-n-1}. \tag{3.33}$$

When $t \to \infty$ then $R \to \infty$ then we obtain

$$|C_2(\infty)|^2 = 2\sinh(\pi\nu)e^{-\pi\nu} = 1 - e^{-2\pi\nu}. \tag{3.34}$$

As $\nu = -in = \frac{\epsilon_{12}^2}{\alpha}$ and for $t = x$ as previously, ν can simplify as

$$\nu = \frac{\epsilon_{12}^2}{\alpha} = \frac{1}{4}\frac{\delta m^2 \sin^2 2\theta}{2E\cos 2\theta \left|\frac{d\ln n_{\rm e}}{dx}\right|_{res}} = \frac{\gamma}{4}. \tag{3.35}$$

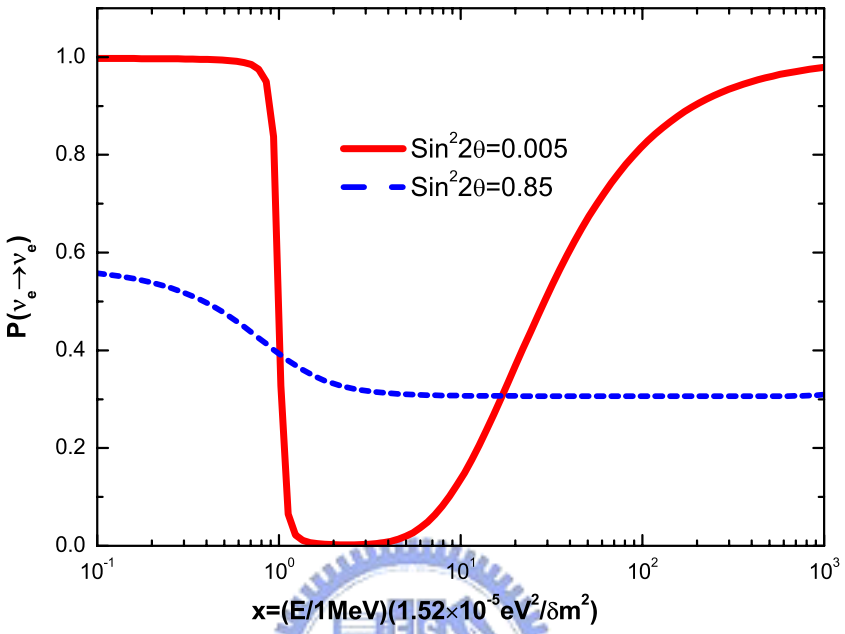

Figure 3.6: The survival probability $P(\nu_e \to \nu_e)$ as function as x for small and large mixing MSW solutions using Eq. (3.23). The $\rho = 100\text{g cm}^{-3}$ is adopted.

Finally, $|C_1(\infty)|^2 = P_{\text{LZ}}=e^{-\frac{1}{2}\pi\gamma}$, in which the γ is dimensionless and is exactly the adiabatic parameter. Thus when $\gamma \gg 1$, $P_{LZ}=0$, and we go back to the adiabatic approximation. The $P_{\text{LZ}}=e^{-\frac{1}{2}\pi\gamma}$ applies only when the variation in density is linear in x. But in case of sun, the density is exponential form, see Eq. (1.5). The Landau-Zener probability should be generalized as

$$P_{LZ} = \frac{\exp[-\pi\gamma F/2] - \exp[-\pi\gamma F/(2S_\theta^2)]}{1 - \exp[-\pi\gamma F/(2S_\theta^2)]}. \tag{3.36}$$

Here, the function F is calculated by Landau's method[12]. When $A \propto r$ then the $F = 1$, and $A \propto \exp(-r)$ then the $F = 1 - \tan^2\theta$. If we apply Eq. (3.23) and (3.36) into the solar neutrino problem we get Fig. 3.6. The

$\gamma F \sim \mathcal{O}(10^2)$ for Sun. In Fig. 3.6, the resonance is at x=1. When $x \gg 1$, and thus $\gamma F \ll 1$, the survival probability approaches the vacuum oscillation. For $x \ll 1$, the $\gamma F \gg 1$, $P_{LZ} \to 0$ and then we recover the adiabatic limit. Therefore, the Landau-Zener probability just apply between them.

3.4 Day-Night Effect

Neutrino propagation in matter must consider the matter effect. This particularly applies to solar electron neutrinos when they pass through earth before reaching the detector in night. The experiments SNO and SKK have found that the flux is different between day and night. The effect of difference between day and night, is called the *Day-Night effect* or *earth effect*.

If we consider the matter effect in earth, the Eq. (3.21) should be modified as

$$P(\nu_e \to \nu_e) = \sum_{i,j=1,2} P_m(\nu_e \to \nu_i) P_{res}(\nu_i \to \nu_j) P_{\oplus}(\nu_j \to \nu_e), \tag{3.37}$$

$$= \left| \begin{pmatrix} 1 & 0 \end{pmatrix} \begin{pmatrix} C^2_{\theta^{\odot}_m} & S^2_{\theta^{\odot}_m} \\ S^2_{\theta^{\odot}_m} & C^2_{\theta^{\odot}_m} \end{pmatrix} \begin{pmatrix} 1-P_{LZ} & P_{LZ} \\ P_{LZ} & 1-P_{LZ} \end{pmatrix} \begin{pmatrix} 1-P_{2e} & P_{2e} \\ P_{2e} & 1-P_{2e} \end{pmatrix} \begin{pmatrix} 1 \\ 0 \end{pmatrix} \right|. \tag{3.38}$$

Here, we donate the symbol $\oplus$ to be earth and $\odot$ to be sun. And we always detect at far away source, then we expand the above matrix after averaging over phase as

$$P(\nu_e \to \nu_e) = \frac{1}{2} + [\frac{1}{2} - (P_{LZ} + \langle P_{2e} \rangle - 2P_{LZ}\langle P_{2e} \rangle)] \cos 2\theta^{\odot}_m. \tag{3.39}$$

The P_{LZ} is given by Eq. (3.36). The $\cos 2\theta^{\odot}_m$ is mixing angle in matter for sun, and is given by Eq. (3.6). And the P_{2e} we shall deriver in appendix B ($P_{1e} = 1 - P_{2e}$), here we just use the result

$$\langle P_{2e} \rangle = S^2_{\theta} + \frac{1}{2} \sin^2 2\theta \frac{A_{\oplus} \delta m^2}{A^2_{\oplus} - 2A_{\oplus}\delta m^2 C_{2\theta} + (\delta m^2)^2}, \tag{3.40}$$

the $\sin^2 2\theta^{\oplus}_m$ is mixing angle in matter for earth.

Fig. 3.7 shows the different path lengths traversed by solar electron neutrinos when they pass through the earth in day and night. In this thesis, we just consider the zenith angle equal to zero. We discuss the day and

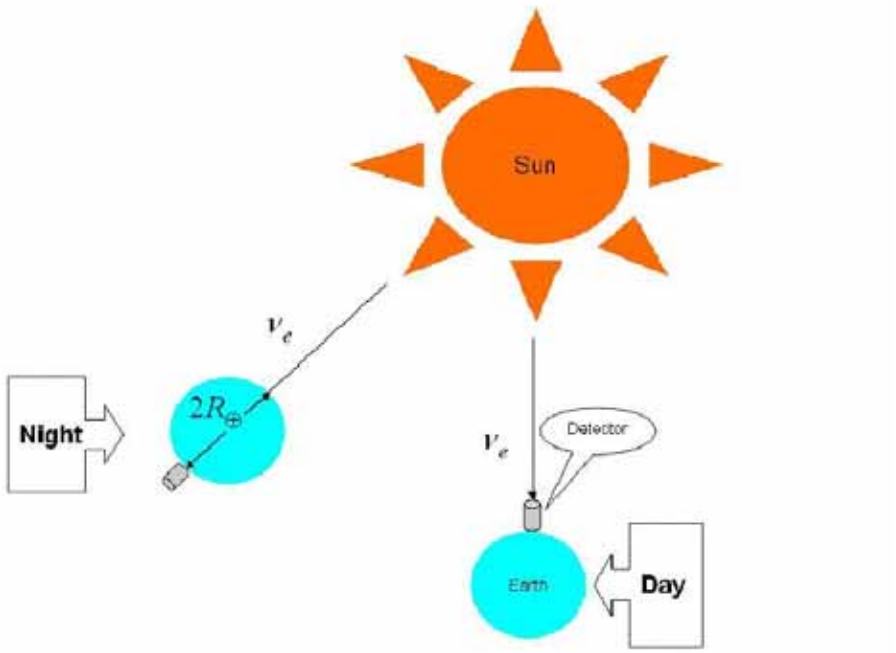

Figure 3.7: This is an illustrative geometry of the solar neutrino propagation during day and night in the earth. $R_\oplus \sim 6.37 \times 10^3$ km denotes the earth radius.

night probability, and apply Eq. (3.23) for day and (3.39) for night to obtain Fig. 3.8. At the neutrinos energy between 10^4 eV$\sim 10^6$ eV, the night probability is almost the same as for the day, because the contribution of the earth effect is small for this region. For energy greater than 10^6 eV, the earth effect emerges. The Day-Night effect provide a chance to check the LMA MSW solution. There are two solution to satisfy Eq. (3.23), one is Large-Mixing-Angle solution and the other is Small-Mixing-Angle. In night, the LMA solution enhance the $P(\nu_e \to \nu_e)$ at high energy. Thus, we can say that we can ignore the SMA solution, because it is not supported by experiments.

In Fig. 3.9, we also show the different density of earth. We see the SMA solution in night was not change with density. For LMA solution, the

probabilities were enhanced by earth-effect. After comparing three kinds of density, we shall get the results that when ρ=5.52 g/cm^3, the enhancement is larger than density in mantle and core.

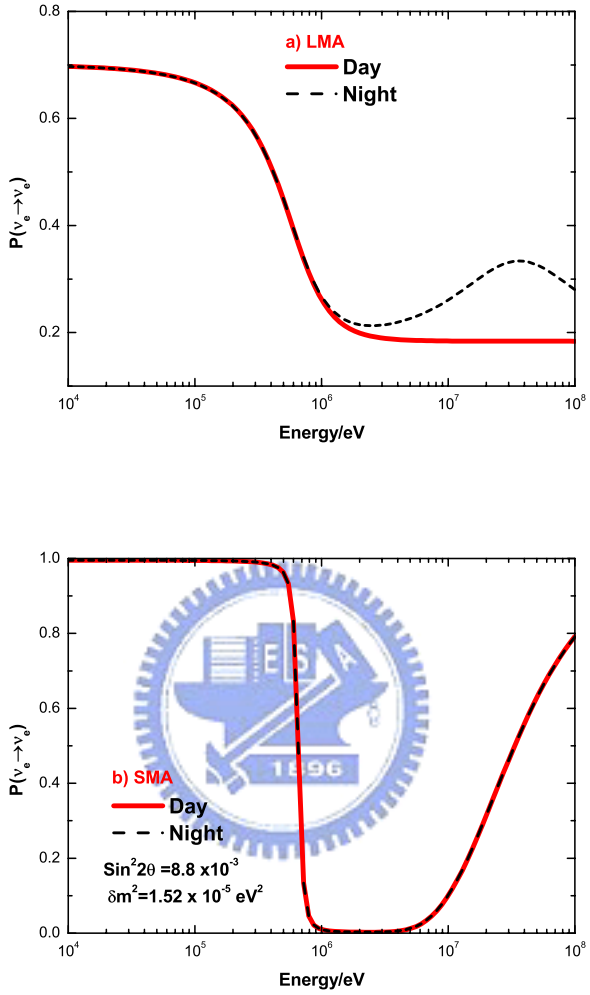

Figure 3.8: The $P(\nu_e \to \nu_e)$ as a function of neutrino energy. Here, a) is SMA solution and b) is LMA solution. The earth effect enhances the probability at high energy in night for a), but nothing change at high energy in night for b). The average density of earth is about 5.52 g/cm^3 and the mixing angle in vacuum we take $\sin^2 2\theta = 8.8 \times 10^{-3}$ for a) and $\sin^2 2\theta = 0.60$ for b). The mass square is equal to 1.52×10^{-5} eV^2. We use Eq. (3.23) for day and (3.39) for night.

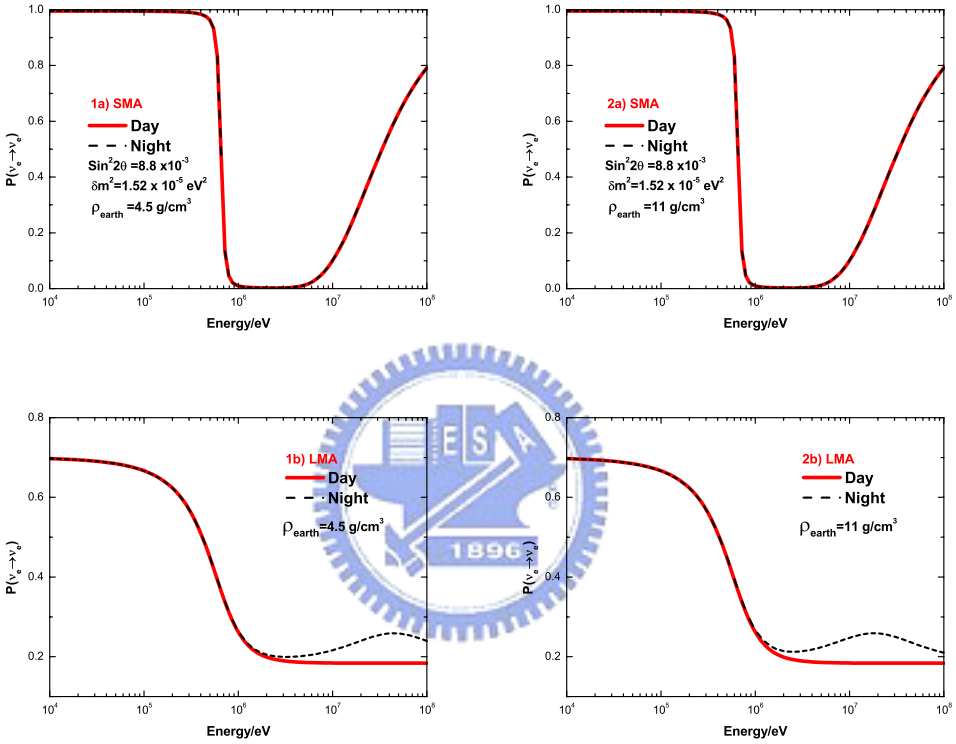

Figure 3.9: We change the density of earth. The density about 4.5 g/cm^3 in the Earth's mantle (1a, 1b) and about 11 g/cm^3 in the core (2a, 2b).

Chapter 4

Predicted Event Rates for Solar Neutrino Experiments

In preceding chapter, we have provided enough basics of neutrinos oscillation theory. Now, we shall use these oscillation results to calculate the event rates, and then we should compare with experiment data. The main method to detect solar neutrinos is using the neutrino interaction with the target. If we know the interaction cross-section, then we can obtain the flux. But the interaction is weak-interaction, so the cross-section is small. That mean the amount of target must be large.

There are two main types of experiments for detection of solar neutrinos[13]. One type is based on neutrino-electron scattering such as Kamiokande, Super-Kamiokande and SNO, the other one is geochemical and radiochemical experiments such as SAGE, GALLEX and Homestake. In this chapter, we shall predict solar electon neutrino event rate for Super-Kamiokande (the neutrino-electron scattering experiment) and Ga experiments (the geochemical and radiochemical experiment).

4.1 Ga Experiments

Two radiochemical solar neutrino experiments using ^{71}Ga are under way, one by a primarily Western European collaboration (GALLEX) and the second is the Russian-American Gallium solar neutrino experiment (SAGE). The GALLEX operated between 1991 and 1997. It used 30 tons of gallium in an aqueous solution and is located in hall A of Gran Sasso Laboratory in Italy.

The SAGE used about 60 tons of gallium metal as a detector target and is in a high mountain in the Baksan Valley in the northern Caucasus Mountains of the Southern Russia.

The neutrino absorption reaction in the gallium experiments is:

$$\nu_e + ^{71}Ga \longrightarrow e^- + ^{71}Ge. \tag{4.1}$$

The threshold for absorption of neutrinos by ^{71}Ga is 0.233 MeV, which is below the maximum energy of the pp reaction (see Fig. 1.2). The predicted capture rate for a ^{71}Ga detector in solar standard model without neutrino oscillation is

$$N_{SSM} = \sum_i \int_{E_{th}}^{E_{max}} \Phi_i(E)\sigma_i(E)dE, \tag{4.2}$$

where the sum extends over the relevant neutrino flux, (i=pp, pep, ^7Be, ^8B, hep) and $E_{th} = 0.233$ MeV. The cross-section $\sigma(E)$ and the flux $\Phi(E)$ are taken from the web site of J. N. Bahcall[4]. We list our result as below:

Source	$\Phi(10^{10}$ cm^{-2}s$^{-1})$	$\sigma(10^{-44}$ cm$^2)$	Ga (SNU)
pp	$5.94(1 \pm 0.01)$	0.117 ± 0.003	66.422
pep	$1.401 \pm 0.02) \times 10^{-2}$	$2.04^{+0.35}_{-0.14}$	2.224
hep	$7.88(1 \pm 0.16) \times 10^{-7}$	714^{+228}_{-114}	0.02
^7Be	$4.86(1 \pm 0.12) \times 10^{-1}$	$0.717^{+0.05}_{-0.021}$	31.824
^8B	$5.82(1 \pm 0.23) \times 10^{-4}$	240^{+77}_{-36}	14.097
Total			114.587

Table 4.1: the Φ is total flux, and the σ is neutrino capture cross sections averaged over the energy spectra[14]. The event rate of Ga we calculated by numerical method.

In order to show the event rates, we introduce a unit SNU (Solar Neutrinos Unit). 1 SNU=10^{-36} times interaction per one target per second. Here we should emphasize the above result is according to the solar standard model. The Ga based experimental result is 74.7±5.13 SNU and is therefore different from SSM result.

We consider "*neutrino oscillations*" to resolve this discrepancy . We use the survival probability given by Eq. (3.23), and we take $\sin^2 2\theta = 0.6$,

$\delta m^2 = 3 \times 10^{-5}$ eV^2 and consider detection in day. Then Eq. (4.2) becomes

$$N_{osc} = \sum_i \int_{E_{th}}^{E_{max}} \Phi_i(E)\sigma_i(E)P(E)dE. \tag{4.3}$$

Substituting various quantity we can obtain the value of N_{osc} as 61.37 SNU. Hence, neutrinos flavor oscillations can explain the experiment.

The ratio of event rate of gallium experiment by theory calculation is

$$R_{th} = \frac{N_{osc}}{N_{SSM}} = 0.54. \tag{4.4}$$

On the other hand, the experimental result divided by solar standard model is

$$R_{exp} = \frac{N_{exp}}{N_{SSM}} = 0.58 \pm 0.06. \tag{4.5}$$

The error $\Delta R = R_{exp} - R_{th}$ is about 0.04 (which is just 6.8%). Thus, we are able to explain the experimental results using *neutrino oscillation*.

4.2 Super-Kamiokande Experiment

It is a $\nu_e - e$ scattering experiment. SKK is Super-Kamiokande in Japan (and SNO is Sudbury Neutrino Observatory in Canada). These are different from neutrino absorption experiments. Here we discuss Super-Kamiokande in some detail as a representative example, where the solar neutrinos are detected using the Cherenkov light emitted by the recoiling electron from neutrino electron elastic scattering. They have the advantages of detecting neutrinos with some information on their time, direction, and energy all simultaneously.

The reaction of neutral current in Fig. 3.1 is

$$\nu + e^- \longrightarrow \nu' + e^-. \tag{4.6}$$

Super-Kamiokande analyzes data above a threshold of 5 MeV of the total energy of the recoil energy[15]. For this threshold energy, we just consider process ^8B and hep. However, according to SSM, the ^8B neutrino flux is larger than hep neutrino flux. So, the contribution of hep flux for Super-Kamiokande could be ignored.

The recoil electrons in Eq. (4.6) are primarily scattered in the forward direction in which the neutrinos are arriving. If solar neutrinos produce scattering events in a detector, reconstruction of electron tracks must determine a vector that points back to the sun.

The predicted capture rate for Super-Kamiokande by standard solar model is [16]

$$N_{SSM} = \int_{E_{emin}}^{E_{emax}} dE_e \int_{m_e}^{\infty} dE_e^{'} f(E_e^{'}, E_e) \int_{E_m}^{E_M} dE \Phi(E) \frac{d\sigma(\nu_e e)}{dT'}. \tag{4.7}$$

In first integral, the $\Phi(E)$ is the standard solar model ^8B neutrino flux with neutrino energy E, and the $\frac{d\sigma(\nu e)}{dT'}$ is the differential cross section of ν-e scattering

$$\frac{d\sigma(\nu e)}{dT'} = \frac{\sigma_0}{m_e} \left[g_L^2 + g_R^2 \left(1 - \frac{T^{'}}{E} \right)^2 - g_L g_R \frac{m_e T^{'}}{E^2} \right], \tag{4.8}$$

$$\begin{aligned} \sigma_0 &= 88 \times 10^{-46} \text{ cm}^2, \\ g_L &= \pm\frac{1}{2} + \sin^2\theta_W, \\ g_R &= \sin^2\theta_W. \end{aligned}$$

The upper sign applies to ν_e-e scattering, the low sign to $\nu_{\nu,\tau}$-e scattering and $\sin^2\theta_W = 0.229$. The E_M and E_m are given as

$$\begin{aligned} E_M &= 15 \text{ MeV (for } ^8\text{B)}, \\ E_m &= \frac{T' + \sqrt{T'^2 + 2m_e T'}}{2}. \end{aligned} \tag{4.9}$$

In second integral, the quantity $f(E_e^{'}, E_e)$ is the energy resolution function of the detector in terms of the physical $(E_e^{'})$ and the measured (E_e), which is given by

$$f(E_e^{'}, E_e) = \frac{1}{\Delta_{T'}\sqrt{2\pi}} \exp\left(-\frac{(T - T^{'})^2}{2\Delta_{T'}^2} \right), \tag{4.10}$$

where $\Delta_{T'}$ is energy resolution at the electron kinetic energy $T^{'}$, and the relation for T and E_e is $E_e = T + m_e$ ($m_e = 0.511$ MeV). The energy resolution function of SKK, we use

$$\Delta_{T'} = 1.6 \text{ MeV}\sqrt{\text{T}'/(10 \text{ MeV})}. \tag{4.11}$$

The lower limit of the first integral is the detector threshold energy, $E_{emin} = E_{SKK}^{threshold} = 5$ MeV and the upper limit is $E_{emax} = 20$ MeV.

Similar to Ga experiment, we should also introduce the oscillation result here. Then, the Eq. (4.7) become

$$N_{osc} = \int_{E_{emin}}^{E_{emax}} dE_e \int_{m_e}^{\infty} dE_e^{'} f(E_e^{'}, E_e) \int_{E_m}^{E_M} dE\Phi(E) \frac{d\sigma_{\nu_{solar}}}{dT'}, \tag{4.12}$$

where $\frac{d\sigma_{\nu_{solar}}}{dT'}$ is given by

$$\frac{d\sigma_{\nu_{solar}}}{dT'} = P(E)\frac{d\sigma(\nu_e e)}{dT'} + [1 - P(E)]\frac{d\sigma(\nu_{\mu,\tau} e)}{dT'}, \tag{4.13}$$

here the $P(E)$ is electron-neutrinos survival probability at the detector. We can also calculate the ratio of the event rate similar to Eq. (4.4) and Eq. (4.5).

The ratio of oscillation and standard solar model is

$$\frac{N_{osc}}{N_{SSM}} = 0.448, \tag{4.14}$$

with the condition $\delta m^2 = 3 \times 10^{-5}$ eV^2 and $\sin^2 2\theta = 0.60$. The experimental result divide by solar standard model for Super-Kamiokande is

$$\frac{N_{exp}}{N_{SSM}} = 0.459 \pm 0.005. \tag{4.15}$$

Using Eq. (4.14) and Eq. (4.15), the error ΔN is 2%. thus, neutrino flavor oscillations of the type $\nu_e \rightarrow \nu_\mu$ can explain the discrepancy for SKK also.

4.2.1 Calculation of Recoil Electron Energy Spectrum

In this thesis, we also calculate the ratio, $R(E_i)$, of the number of observed events, N_i^{obs} in a given energy bin E_i, to the number, N_i^{SSM}, expected from the solar standard model, where

$$R(E_i) = \frac{N_i^{obs}}{N_i^{SSM}}. \tag{4.16}$$

Then, we can rewrite Eq. (4.12) as

$$N_i^{osc} = \int_{E_i}^{E_i + m_e} dE_e \int_{m_e}^{\infty} dE_e^{'} f(E_e^{'}, E_e) \int_{E_m}^{E_M} dE\Phi(E) \frac{d\sigma_{\nu_{solar}}}{dT'}, \tag{4.17}$$

here, every parameter was defined as before, and for the N_i^{SSM} we just set $P(E) = 1$, and the E_i is any energy in spectrum. We apply these result to produce the figures that follow.

In Fig. 4.1, we show the δm^2 and $\sin^2 2\theta$ both for SKK and SNO. The comparison between theoretical prediction and experimental data are quite different. The vacuum oscillation alone thus tend to fail to explain the data. In Fig. 4.2 a) and Fig. 4.2 b), we compare with LMA solution and SMA solution in day time. The figure indicates that, the LMA is much better then SMA. And Fig. 4.3 show as the night effect for LMA and SMA. The SMA fail to explain the night effect also. We show the day and night event rate for LMA respectively in the Fig. 4.4. The figure show that LMA can explain both the day and night effect.

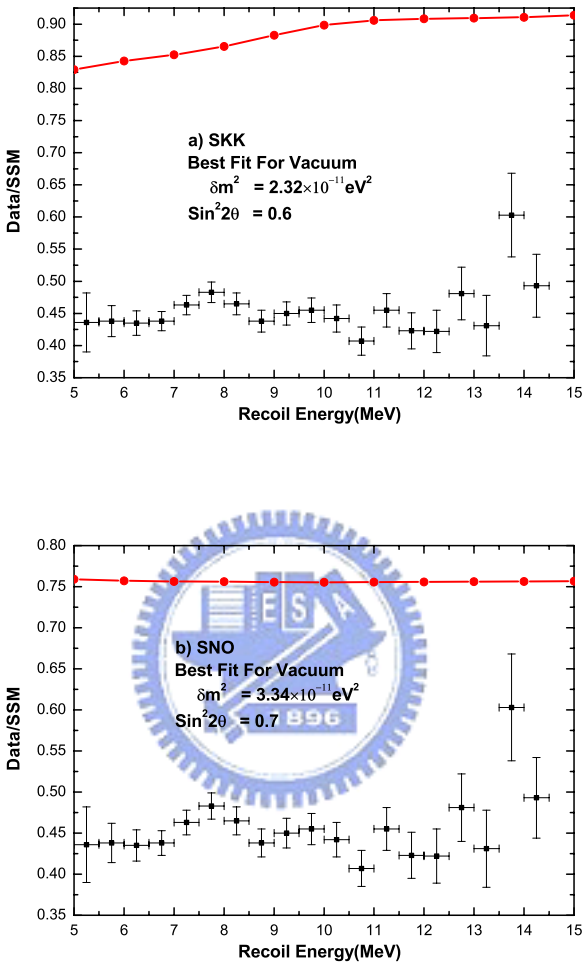

Figure 4.1: The best fit electron recoil energy spectrum for vacuum oscillation and its comparison with SKK and SNO experiments. We use Eq. (2.13), here the SKK data is for 1258 days and is taken from Ref.[17]. The $\sin^2 2\theta$ and δm^2 in Fig. 4.1 a), are taken from Eq. (2.20). For Fig. 4.1 b), we use Eq. (2.21).

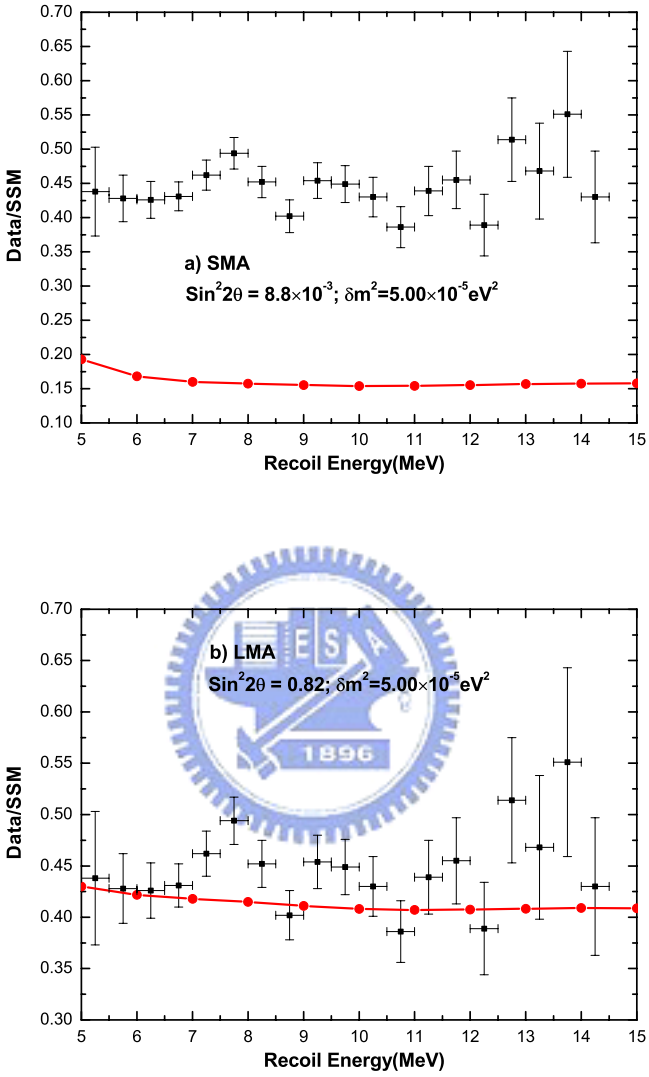

Figure 4.2: The comparison between the MSW solutions and the data a) for MSW (SMA), b) for MSW (LMA) in day time. Eq. (3.23) is used here. The data is for 1258 days for SuperKamiokande experiment [17]. Note that the MSW (LMA) explain the data batter than MSW (SMA).

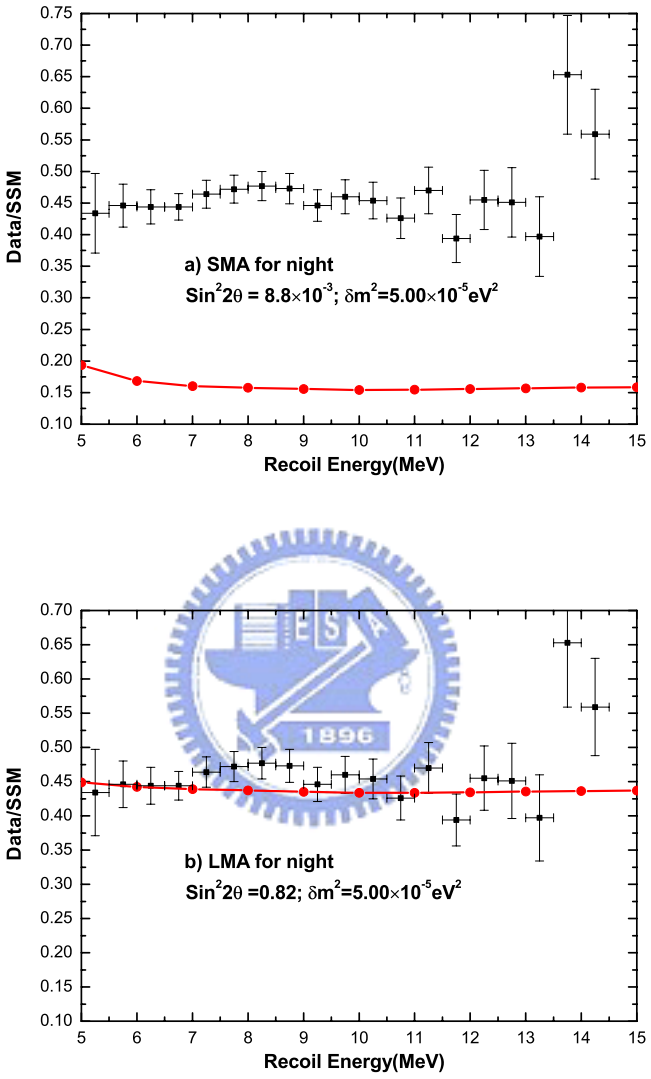

Figure 4.3: This is LMA and SMA comparison for night. The survival probability for night is given by Eq. (3.39). The experimental data is for 1258 days of SuperKamiokande observations [17].

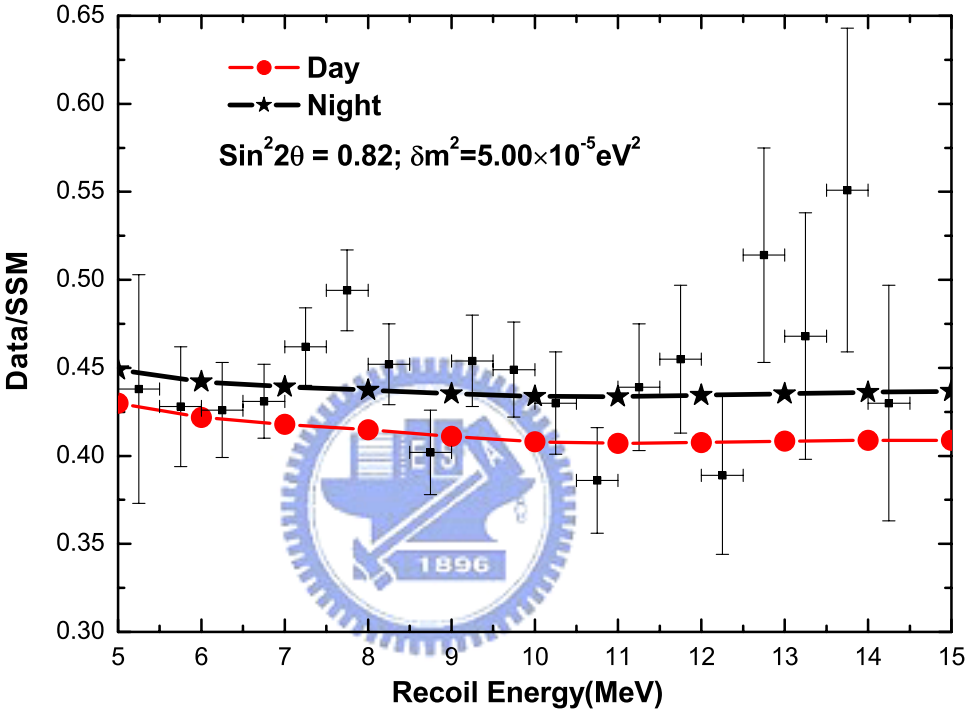

Figure 4.4: The Day-Night Spectrum Test. Here, we used LMA solution, and Eq. (3.23) for survival probability in day and Eq. (3.39) in night. At high energy, the earth effect enhance events in night, (see Fig. 3.8 also). The experimental data is take from Ref.[17].

Chapter 5

Results and Discussion

The solar electron neutrino flux is less than the predicted one in the standard solar model. Our Eq. (4.4) and Eq. (4.5) indeed confirm this. In this thesis, assuming that the solar neutrinos undergo $\nu_e \rightarrow \nu_\mu$ transitions, we have treated the solution of solar neutrino problem step by step.

First, we make the assumption that the background condition in which neutrinos are propagating is vacuum. The relevant oscillation probability expression is discussed in chapter 2. This result tell us that the oscillation length is very important for explaining the observed solar ν_e deficit. For solar neutrinos, the oscillation length is comparable to the distance between the sun and the earth, if $\delta m^2 \simeq 10^{-11}$ eV^2. Fixing the oscillation length, we can estimate the range of neutrino mixing parameters to explain the various experimental results. In this thesis, we have applied this procedure for the latest SKK as well as the SNO results. Eq. (2.20) gives the range of the two neutrino mixing parameters for the SKK experiment, whereas Eq. (2.21) gives the same for the SNO experiment.

Next, we turn to more realistic situation. We consider the effects of neutrino interactions for a system of mixed neutrinos during their propagation in chapter 3. This leads us to corrections in the vacuum result. This includes the analytic description of the process that involve the neutrino propagation inside the sun. The Mikheyev Smirnov Wolfenstein (MSW) effect is introduced including its Landau-Zener correction. For a resonance occurring inside the sun, the Landau-Zener effect shall enhance the solar electron neutrino survival probability obtained under the MSW approximation. Two types of solutions within the MSW effect are found to explain the experimental results. These are called the Large Mixing Angle (LMA) solution and the

Small Mixing Angle (SMA) solution.

The next step to the solve neutrino problem in this thesis is to study the Day-Night effect. The analytic description of this effect is given in chapter 3. The experiments have found that the solar ν_e flux is different in day w.r.t to that in night for neutrino energy greater than 1 MeV. We consider the solar neutrino survival probability at mid night and compare it with the one in mid day (Fig. 3.8). We find that the survival probability at the night with LMA solution is compatible with the experimental observations. It thus excludes the SMA solution.

We also calculate the solar electron neutrino event rates for the two main type of experiments. To do this, parameterizations for the solar neutrino flux, and the neutrino nucleon/electron cross section were found first. These are then convolved with the solar electron neutrino survival probability obtained in previous chapters. Our results are given by Eq. (4.4) and Eq. (4.14) in chapter 4. These are then compared with the observations also. As a last observable, the recoil electron energy spectrum for SKK experiment is also calculated in chapter 4. We depict results for our calculation of the recoil electron energy spectrum in Fig. 4.1 to Fig. 4.4 along with experimental observations.

In summary, the $\nu_e \to \nu_\mu$ neutrino flavor oscillation channel with neutrino mixing parameters ($\sin^2 2\theta$, δm^2)= (0.81, 5×10^{-5} eV^2) is found to be the most favorable to explain all the solar neutrino diagnostic measurements. These include the average flux in Ga, SNO and SKK experiments, the recoil electron energy spectrum and the day night effect in SKK.

Appendix A

How to Solve the Weber Equation

A.1 The Weber Equation

When we study Landau-Zener Probability we encounter some difficulty, especially for Weber Eq. $\frac{d^2U(z)}{dz^2} + (n - \frac{z^2}{4} + \frac{1}{2})U(z) = 0$ given by Eq. (3.31).

Below we provide some details of its solution. Then we apply Weber Function to solve for Landau-Zener Formula.

Consider differential equation of the form

$$\frac{d^2\omega}{dx^2} = f(x)\omega, \tag{A.1}$$

in which x is a real or complex variable, and $f(x)$ a prescribed function. All homogeneous linear differential equation of the second order can be put in this form by appropriate change of dependent or independent variable.

But above equation we do not know how to solve exactly. Then we use a tricky way to solve to it. That is, make Eq. (A.1) of the form [18]

$$\frac{d^2\varpi}{d\xi^2} = (1 + \phi)\varpi. \tag{A.2}$$

If ϕ is enough small then we can neglect it. Then the solution of Eq. (A.2) can approach to $\varpi = Ae^{\xi} + Be^{-\xi}$. Here we can let

$$\varpi = \{\xi'(x)\}^{\frac{1}{2}}\omega. \tag{A.3}$$

Then ϖ satisfies

$$\frac{d^2\varpi}{d\xi^2} = \{\dot{x}^2 f(x) + \dot{x}^{\frac{1}{2}} \frac{d^2 \dot{x}^{-\frac{1}{2}}}{d\xi^2}\}\varpi, \tag{A.4}$$

where dots signify differentiations with respect to ξ.

We can compare with Eq. (A.2) and Eq. (A.4). We compromise by choosing $\xi(x)$ so that the term $\dot{x}^2 f(x)$ is a constant, which we take to be unity. Thus

$$\xi(x) = \int_{0^+}^{x} f^{\frac{1}{2}}(x')dx'. \tag{A.5}$$

Until now, we get the solution of Eq. (A.4) as

$$\varpi \cong Ae^{\int_{0^+}^{x} f^{\frac{1}{2}}(x')dx'} + Be^{-\int_{0^+}^{x} f^{\frac{1}{2}}(x')dx'}.$$

In terms of ω, we obtain

$$\omega = \{\xi'(x)\}^{\frac{-1}{2}}\varpi \cong Af^{\frac{-1}{4}} e^{\int_{0^+}^{x} f^{\frac{1}{2}}(x')dx'} + Bf^{\frac{-1}{4}} e^{-\int_{0^+}^{x} f^{\frac{1}{2}}(x')dx'}. \tag{A.6}$$

Eq. (A.6) we call Liouville-Green Function.

A.2 Relevance of Weber Equation for P_{LZ}

The Eq. (A.1) can be write in the form

$$\frac{d^2\omega}{dx^2} = (\frac{1}{4}x^2 + a)\omega, \tag{A.7}$$

as we take $f = \frac{1}{4}x^2 + a$, then using Eq. (A.5)

$$\xi(x) = \int_{0^+}^{x} (\frac{1}{4}x'^2 + a)^{\frac{1}{2}} dx'. \tag{A.8}$$

For large x, 0^+ is plus time and approach to zero. Thus

$$\xi = \frac{1}{4}x^2 + a\ln x + constant + O(x^{-2}). \tag{A.9}$$

Hence the principal solution $U(a,x)$ is specified by the condition

$$U(a,x) \sim x^{-a-(\frac{1}{2})} e^{-\frac{x^2}{4}}, \tag{A.10}$$

when $x \to +\infty$. We also denote $U(a,x)$ by $D_{-a-\frac{1}{2}}(x)$.

Now Eq. (3.31) is

$$\frac{d^2U(z)}{dz^2} + \left(n - \frac{z^2}{4} + \frac{1}{2}\right)U(z) = 0. \tag{A.11}$$

Where $z = \sqrt{\alpha}e^{-i\frac{\pi}{4}}t$ and $n = i\frac{\epsilon_{12}^2}{\alpha}$. We apply Eq. (A.10) here. We get $U_+(z) \sim z^{-n-1}e^{\frac{z^2}{4}}$ and $U_-(z) \sim z^n e^{\frac{-z^2}{4}}$ but we want to know probability when time is positive infinite. Because probability must be converge so the solution $U_+(z)$ must be dropped. As a result, we get back Eq. (3.32).

Appendix B

Derivation of the P_{2e} in Day-Night effect

Here we discuss the problem of finding P_{2e}. The $A_{\oplus}$ donate the shift potential became of interaction with matter in earth, and we assume the density of earth is constant. Therefore, the neutrino propagation in earth is

$$i\frac{d}{dx}\begin{pmatrix}\nu_1\\ \nu_2\end{pmatrix} = \frac{1}{2E}\left[\begin{pmatrix}m_1^2 & 0\\ 0 & m_2^2\end{pmatrix} + U^{\dagger}\begin{pmatrix}A_{\oplus} & 0\\ 0 & 0\end{pmatrix}U\right]\begin{pmatrix}\nu_1\\ \nu_2\end{pmatrix}. \tag{B.1}$$

The U matrix is define as Eq. (2.8), then we can obtain the Hamiltonian in the mass-eigenstate

$$H_m = \frac{1}{2E}\begin{pmatrix}m_1^2 + A_{\oplus}C_{\theta}^2 & A_{\oplus}S_{\theta}C_{\theta}\\ A_{\oplus}S_{\theta}C_{\theta} & m_2^2 + A_{\oplus}S_{\theta}^2\end{pmatrix}. \tag{B.2}$$

Here, we neglects non-important term. Adding a phase factor still unaffect the probability P_{2e}. So, we can rewrite the Hamiltonian as

$$H_m = \frac{1}{2E}\begin{pmatrix}m_1^2 + A_{\oplus}C_{\theta}^2 - \frac{1}{2}Tr(H_m) & A_{\oplus}S_{\theta}C_{\theta}\\ A_{\oplus}S_{\theta}C_{\theta} & m_2^2 + A_{\oplus}S_{\theta}^2 - \frac{1}{2}Tr(H_m)\end{pmatrix}. \tag{B.3}$$

Or in terms of Pauli-matrices

$$\begin{aligned} H_m &= \frac{1}{4E}\begin{pmatrix}-\delta m^2 + A_{\oplus}C_{2\theta} & A_{\oplus}S_{2\theta}\\ A_{\oplus}S_{2\theta} & \delta m^2 - A_{\oplus}C_{2\theta}\end{pmatrix},\\ &= \frac{1}{4E}\left[A_{\oplus}S_{2\theta}\cdot\sigma_1 + (-\delta m^2 + A_{\oplus}C_{2\theta})\sigma_3\right],\\ &= (\mathbf{a}\cdot\sigma). \end{aligned} \tag{B.4}$$

The Pauli-matrices and **a** vector are defined as

$$\sigma_1 = \begin{pmatrix} 0 & 1 \\ 1 & 0 \end{pmatrix}, \quad \sigma_2 = \begin{pmatrix} 0 & -i \\ i & 0 \end{pmatrix}, \quad \sigma_3 = \begin{pmatrix} 1 & 0 \\ 0 & -1 \end{pmatrix}, \tag{B.5}$$

$$\mathbf{a} = \frac{1}{4E} \begin{pmatrix} A_\oplus S_{2\theta} \\ 0 \\ -\delta m^2 + A_\oplus C_{2\theta} \end{pmatrix}.$$

The time evolution operator is given by

$$\mathcal{T}(t) = \exp(-iHt). \tag{B.6}$$

Now, we have two properties[19] of Pauli-matrices to obtain time-evolution function

$$\begin{aligned} (\mathbf{a}\cdot\sigma)^2 &= \mathbf{a}^2, \\ \mathcal{T}(t) = \exp(-i\mathbf{a}\cdot\sigma t) &= \mathbf{1}\cos(at) - i\frac{\mathbf{a}\cdot\sigma}{a}\sin(at). \end{aligned} \tag{B.7}$$

Thus, we may easily calculate the amplitude $\mathcal{A}_{2e}$=$\langle\nu_e|\nu_2(L)\rangle$ by using the the explicit form of the Pauli-matrices. Combining the result of Eq. (2.8) and Eq. (B.7) we obtain

$$\mathcal{A}_{2e} = \langle\nu_2|\sin\theta\,\mathcal{T}(L)|\nu_2\rangle. \tag{B.8}$$

L is the length of neutrino propagation. From which we can get the probability

$$\begin{aligned} P_{2e} &= |\mathcal{A}_{2e}|^2, \\ &= S_\theta^2 + \sin^2 2\theta \frac{A_\oplus \delta m^2}{A_\oplus^2 - 2A_\oplus \delta m^2 C_{2\theta} + (\delta m^2)^2}\sin^2(aL), \end{aligned} \tag{B.9}$$

$$\tag{B.10}$$

with

$$a = \frac{1}{4E}\sqrt{(A - \delta m^2 C_{2\theta})^2 + \delta m^2 S_{2\theta}^2}. \tag{B.11}$$

The average probability using above equation is

$$\langle P_{2e}\rangle = S_\theta^2 + \frac{1}{2}\sin^2 2\theta \frac{A_\oplus \delta m^2}{A_\oplus^2 - 2A_\oplus \delta m^2 C_{2\theta} + (\delta m^2)^2}. \tag{B.12}$$

It is the same as Eq. (3.40).

Bibliography

[1] M. Fukugita and A. Suzuki, *Physics And Astrophysics Of Neutrinos*, Tokyo, Japan: Springer (1994) 934 p.

[2] R. N. Mohapatra and P. B. Pal, *Massive Neutrinos In Physics And Astrophysics, Second Edition*, World Sci. Lect. Notes Phys. **60**, 1 (1998) [World Sci. Lect. Notes Phys. **72**, 1 (2004)].

[3] J. N. Bahcall and R. K. Ulrich, *Solar Models, Neutrino Experiments And Helioseismology*, Rev. Mod. Phys. **60**, 297 (1988).

[4] Homepage of J.N. Bahcall, http://www.sns.ias.edu/jnb/.

[5] J. N. Bahcall and M. H. Pinsonneault, *What do we (not) know theoretically about solar neutrino fluxes?*, Phys. Rev. Lett. **92**, 121301 (2004) [arXiv:astro-ph/0402114].

[6] T. K. Kuo and J. Pantaleone, *Neutrino Oscillations In Matter*, Rev. Mod. Phys. **61**, 937 (1989).

[7] K. Hagiwara *et al.* [Particle Data Group Collaboration], *Review Of Particle Physics*, Phys. Rev. D **66**, 010001 (2002).

[8] Q. R. Ahmad *et al.* [SNO Collaboration], *Direct evidence for neutrino flavor transformation from neutral-current interactions in the Sudbury Neutrino Observatory*, Phys. Rev. Lett. **89**, 011301 (2002) [arXiv:nucl-ex/0204008].

[9] L. Wolfenstein, *Neutrino Oscillations In Matter*, Phys. Rev. D **17**, 2369 (1978).

[10] S. P. Mikheyev and A. Yu. Smirnov, *Resonant Neutrino Oscillations In Matter*, Prog. Part. Nucl. Phys. **23**, 41 (1989).

[11] C. Zener, *Nonadiabatic Crossing Of Energy Levels*, Proc. Roy. Soc. Lond. A **137**, 696 (1932).

[12] T. K. Kuo and J. Pantaleone, *Nonadiabatic Neutrino Oscillations In Matter*, Phys. Rev. D **39**, 1930 (1989).

[13] C. Giunti and M. Laveder, *Essential solar neutrinos*, arXiv:hep-ph/0301276.

[14] J. N. Bahcall and C. Pena-Garay, *Solar models and solar neutrino oscillations*, arXiv:hep-ph/0404061.

[15] M. B. Smy [Super-Kamiokande collaboration], *Solar neutrino precision measurements using all 1496 days of Super-Kamiokande-I data*, Nucl. Phys. Proc. Suppl. **118**, 25 (2003) [arXiv:hep-ex/0208004].

[16] J. N. Bahcall, P. I. Krastev and A. Y. Smirnov, *Is large mixing angle MSW the solution of the solar neutrino problems?*, Phys. Rev. D **60**, 093001 (1999) [arXiv:hep-ph/9905220].

[17] S. Fukuda *et al.* [Super-Kamiokande Collaboration], *Solar ^8B and hep neutrino measurements from 1258 days of Super-Kamiokande data*, Phys. Rev. Lett. **86**, 5651 (2001) [arXiv:hep-ex/0103032].

[18] Frank W.J. Olver, *Asymptotics and special functions, AKP Classics* (1997).

[19] J. J. Sakurai, *Modern Quantum Mechanics (2nd Edition)*.